Detectors of Cosmic Rays Gamma-Rays and Neutrinos

(I)

G. Navarra
University – INFN
Torino – Italy

Third School on Cosmic Rays and Astrophysics
August 25 to September 5, 2008
Arequipa - Perú

(I)

- Introduction
- Something about historical detectors
- Space detectors

Our aims:

PARTICLE IDENTIFICATION

ENERGY MEASUREMENTS

ARRIVAL DIRECTIONS

TIME VARIATIONS

Wide range of energies:

- Dark matter 10^3 eV
- Solar/SN neutrinos 10^6 eV
- Gamma-rays $10^3 – 10^{12}$ eV … 10^{21} eV
- Charged CR: 10^6 eV – 10^{21} eV
- C. neutrinos … 10^{21} eV

Wide quality of detectors

- -dE/dx
- Secondary/cascade measurements
- Magnetic deflection
- Cherenkov
- Acoustic
- Radio

Wide range of dimensions

- dark matter / space detectors (< m)
  LE neutrinos (10 – 100 m)
- “sampling arrays”
  Acceptance area >> sensitive area
  (Auger: 3000 km^2 vs 16000 m^2… factor 200000!)
  Shower detectors
- Extensive Air Showers (HE CRs, Gamma rays)
- Underwater/ice neutrino (km)

Wide range of locations

- Space
- Ground based
- … sea level… mountain… “deserts”
- Underground
- Underwater
- Under-ice / on-ice

+ long duration, stable observations

+ sensitivity to bursts

DIRECT/NON-DIRECT observations

- DIRECT : the particle under study interacts in your detector: you can measure the particle itself or its products (as for photons)

- NON-DIRECT: the secondaries produced by the particle are detected: typical of ground based charged particle experiments

THE EARTH ATMOSPHERE

ATMOSPHERIC
PRESSURE

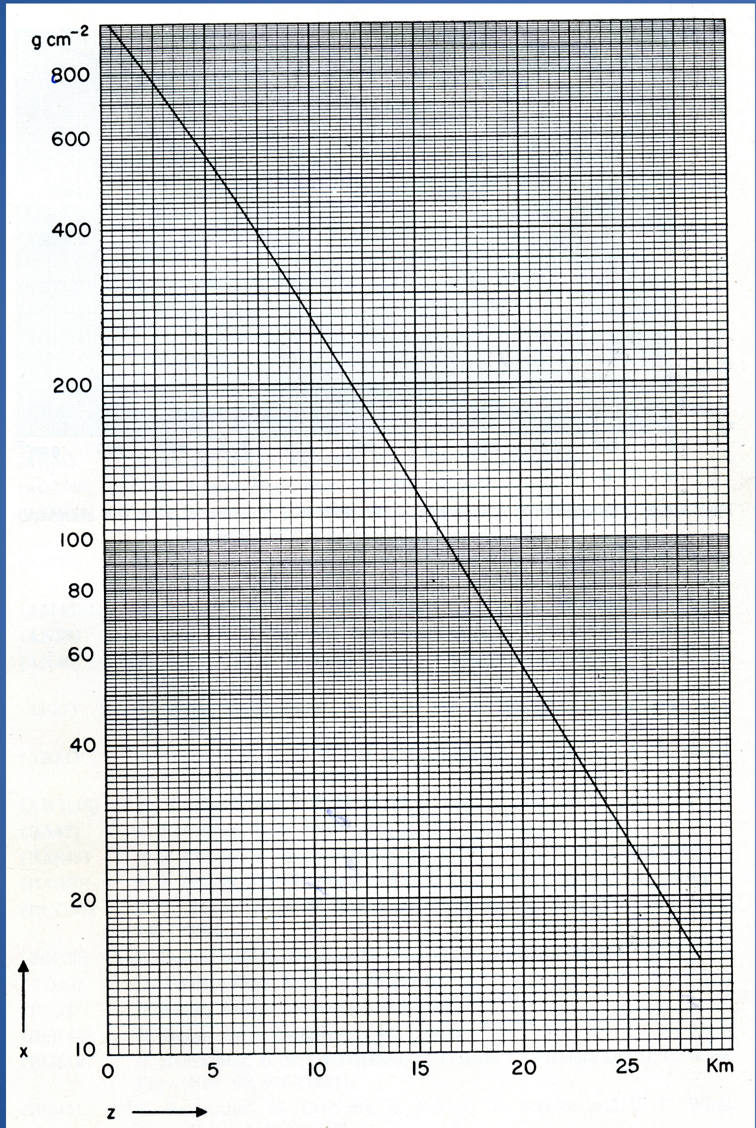

ALTITUDE A.S.L.

THE EARTH ATMOSPHERE

x 10^{10} TeV neutrinos m.f.p.

ATMOSPHERIC PRESSURE

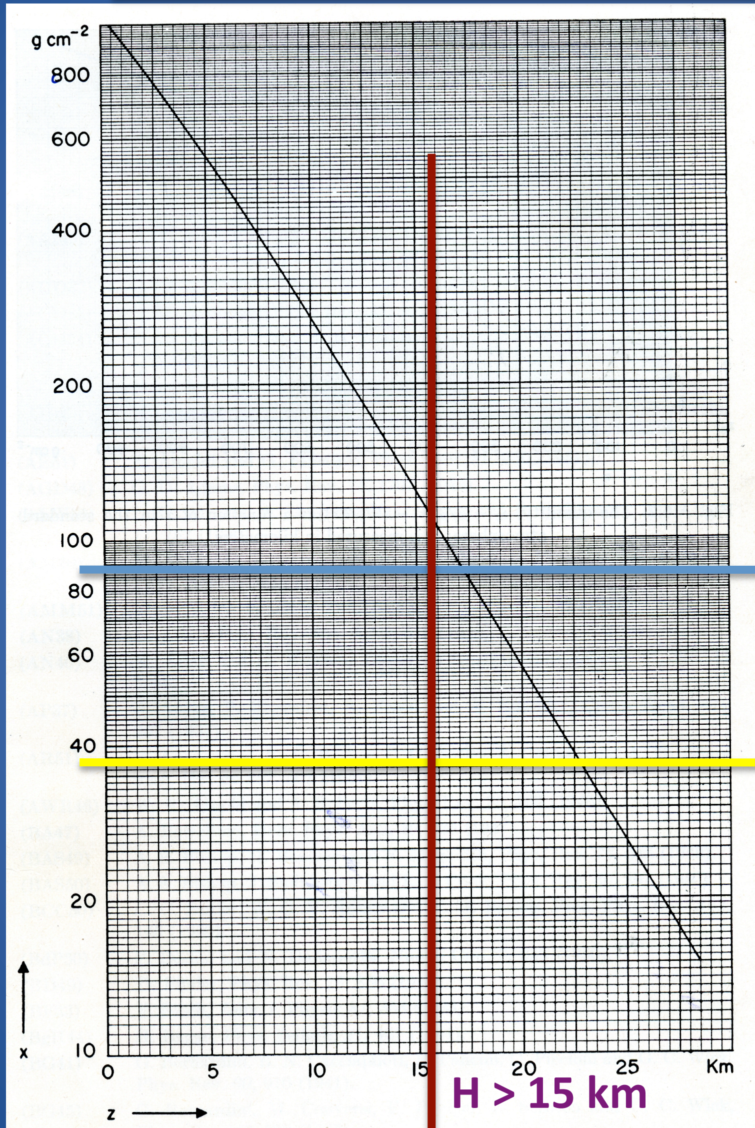

Proton m.f.p. (hadronic int.)

Photon m.f.p. (pair production)

ALTITUDE A.S.L.

A few words on history…

- Detectors and methods

Why…

- to start with the basis of our detectors
- and also to stress the “globality” of CR detectors and remind that these methods are ready to be applied on different scales

THE DISCOVERY OF COSMIC RAYS

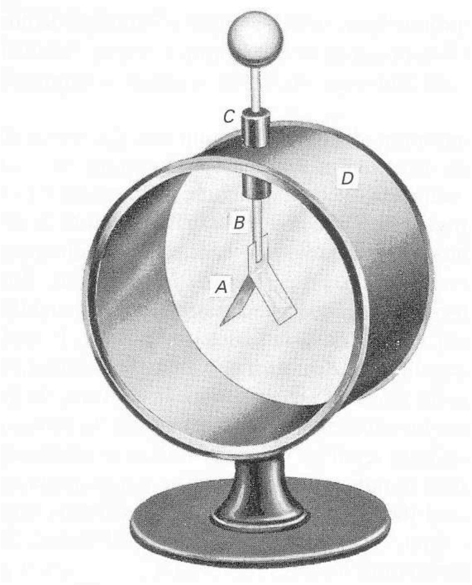

COLLECTIVE DETECTOR

The electroscope

When electroscope is charged, the leaves (A) are pushed apart
The ionization of the gas inside discharge the electroscope and the leaves move towards each other.
The rate at which the leaves came together measured the amount of ionization.

Spontaneous discharge of the electroscope !

1901 Wilson: the discharge is identical on the ground and in a tunnel
X-rays and radioactive substances discharged the electroscopes
Rutherford: this is due to the natural radioactivity
1912 V. Hess: COSMIC RAYS

THE DISCOVERY OF COSMIC RAYS

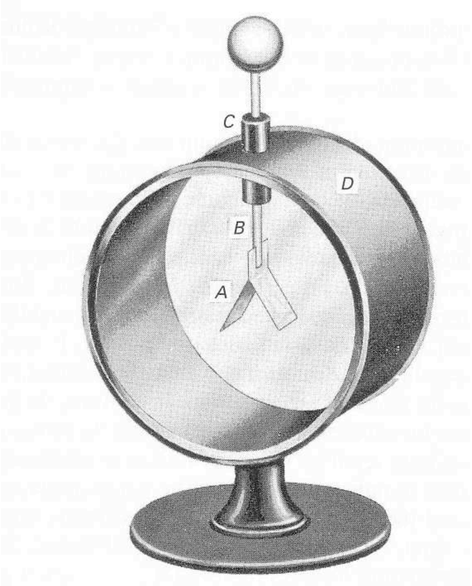

COLLECTIVE DETECTOR

The electroscope

When electroscope is c
pushed apart
The ionization of the ga
electroscope and the le
The rate at which the le
the amount of ionizatio

Spontaneous discharge o

1901 Wilson: the discha
and in a tunnel
X-rays and radioactive s
electroscopes
Rutherford: this is due
1912 V. Hess: COSMIC RAYS

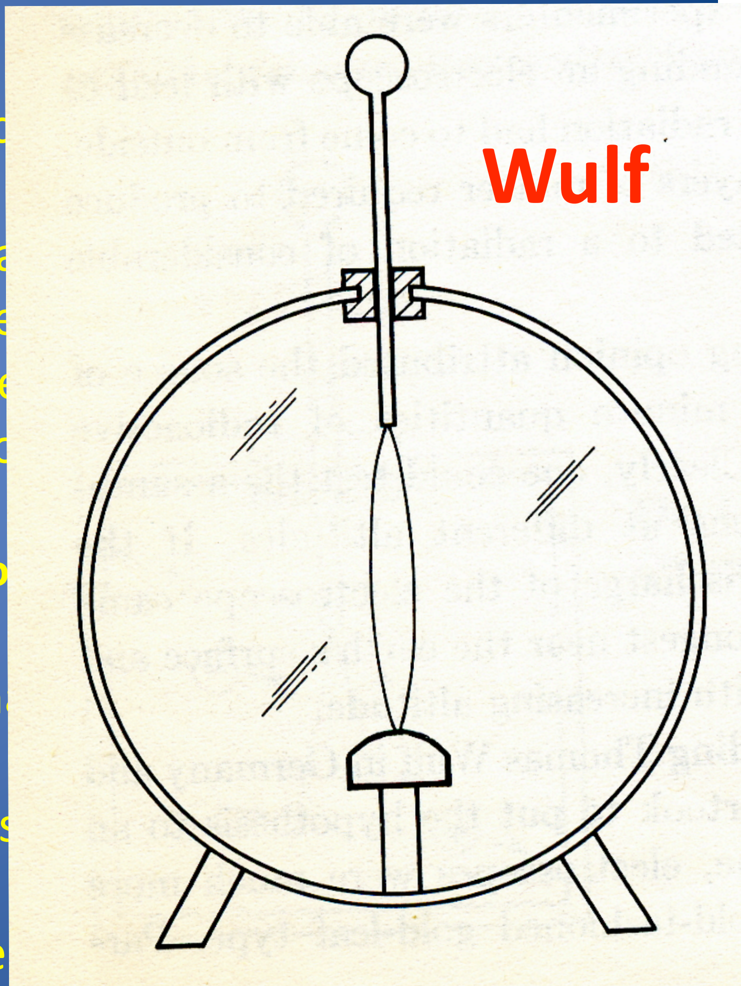

Fig. 1-3
develop
used in
ments o

Geiger: the *point counter*

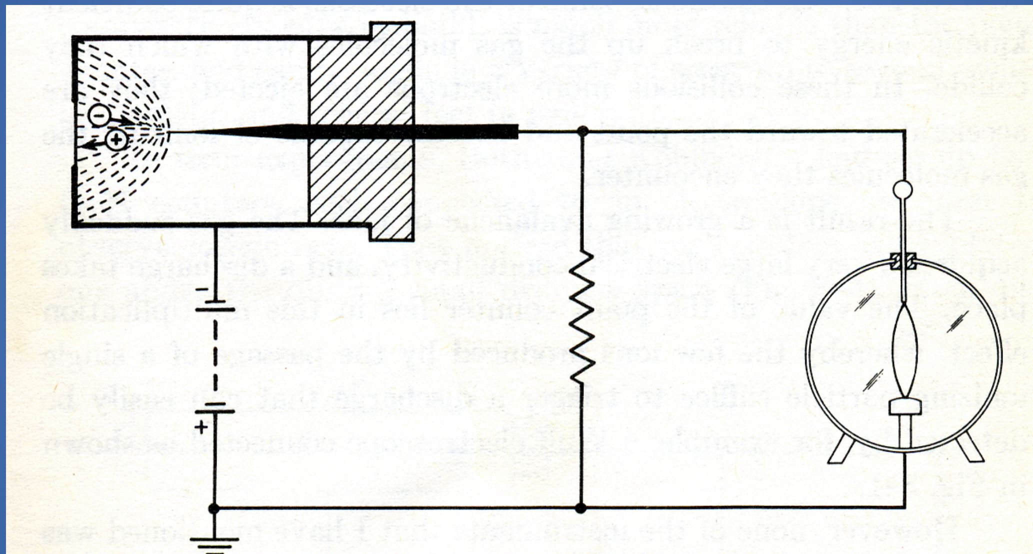

1929 ==> Geiger-Muller counter, avalanche

SINGLE PARTICLE DETECTOR

Coincidence:
Bothe and Kohlhoerster

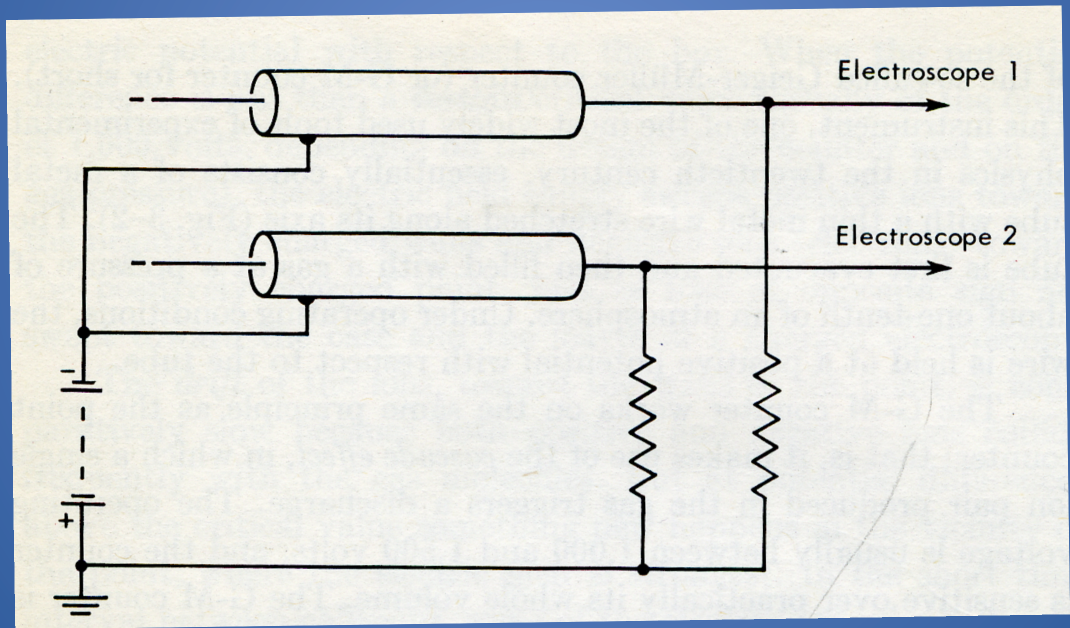

(Field of views, directions, particle penetration, trigger)

The coincidence circuit
B. Rossi

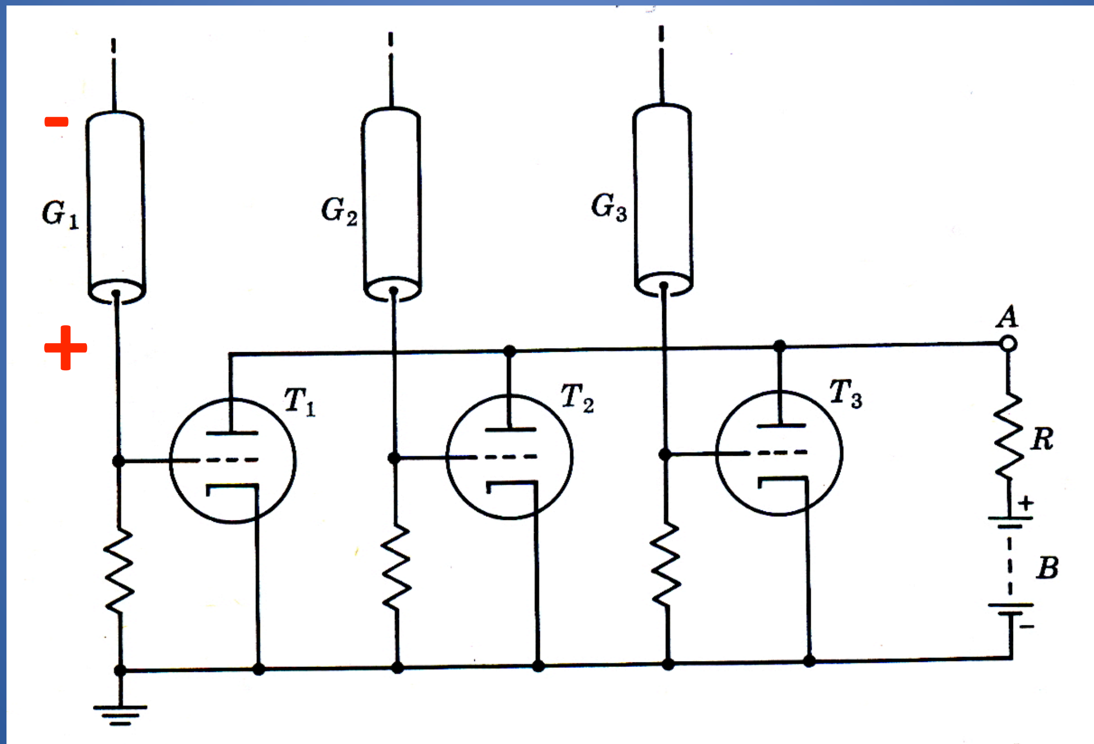

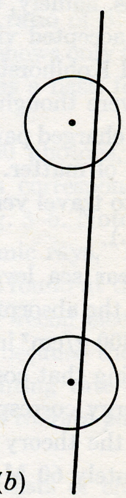

(b)

d-particle coincidences. (a) A photon produces a

Earth magnetic field

E [eV] = 300 B Rc [gauss cm]

B geomagnetic field

Rc radius of Earth

$(B\ Rc)_E = 0.32 \times 6.4\ 10^8 = 2\ 10^8$ gauss cm

$E_E = 300 \times 2\ 10^8$ [eV] = 60 GeV

Particles with $E < E_E$ can be affected by Earth

$\gamma_E = 300\ (Z_e/M_{eV})$ B Rc [gauss cm]

Earth environment as a magnetic analyzer

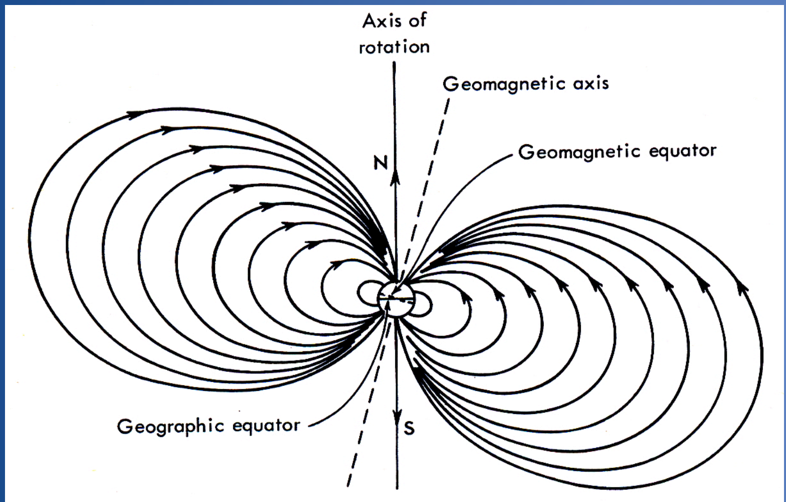

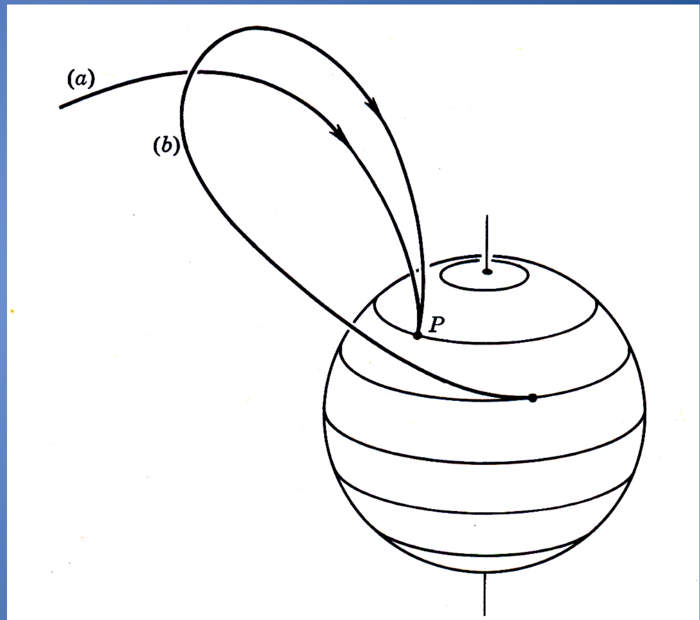

Allowed and forbidden directions

Atmosphere as a magnetic analyzer
latitude effect
CR charged particles

Allowed and forbidden directions

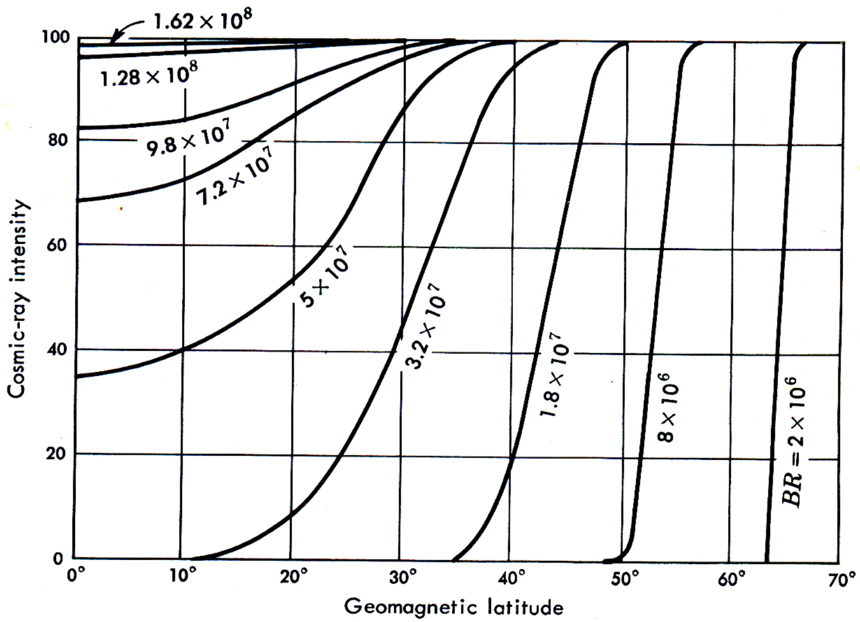

Clay 1927 Leiden-Java Compton

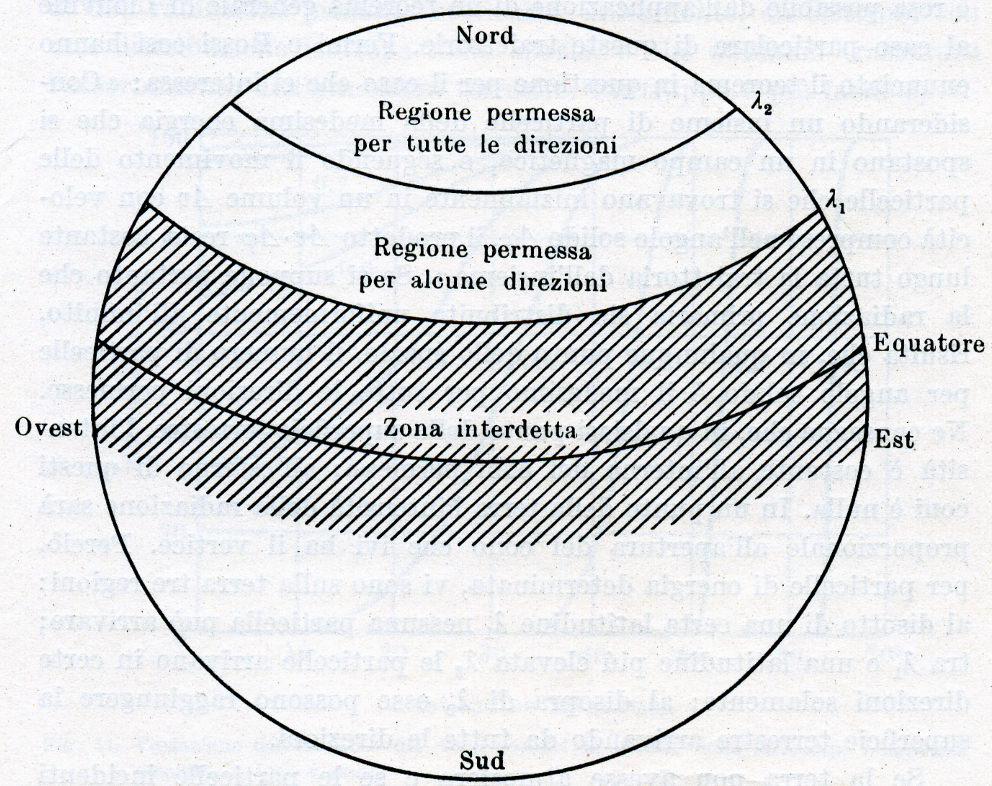

Fig. 50. Date delle particelle di una certa energia, esse non potranno raggiungere la Terra che alle latitudini maggiori di λ_1. Al di sopra di λ_2 tutte potranno raggiungere la Terra, qualunque sia la loro direzione. Tra λ_1 e λ_2 solamente quelle la cui direzione è contenuta in un certo cono (aperto verso l'ovest per le positive, e verso l'est per le negative) potranno raggiungere la Terra.

Atmosphere as a magnetic analyzer
CR dominated by positive charges

E-W effect 1933

Johnson+Alvarez
Mexico City 29 deg North
10% @ 45 deg
Rossi + De Benedetti
Asmara 11 dg North 26%
Excess from West ==> positive

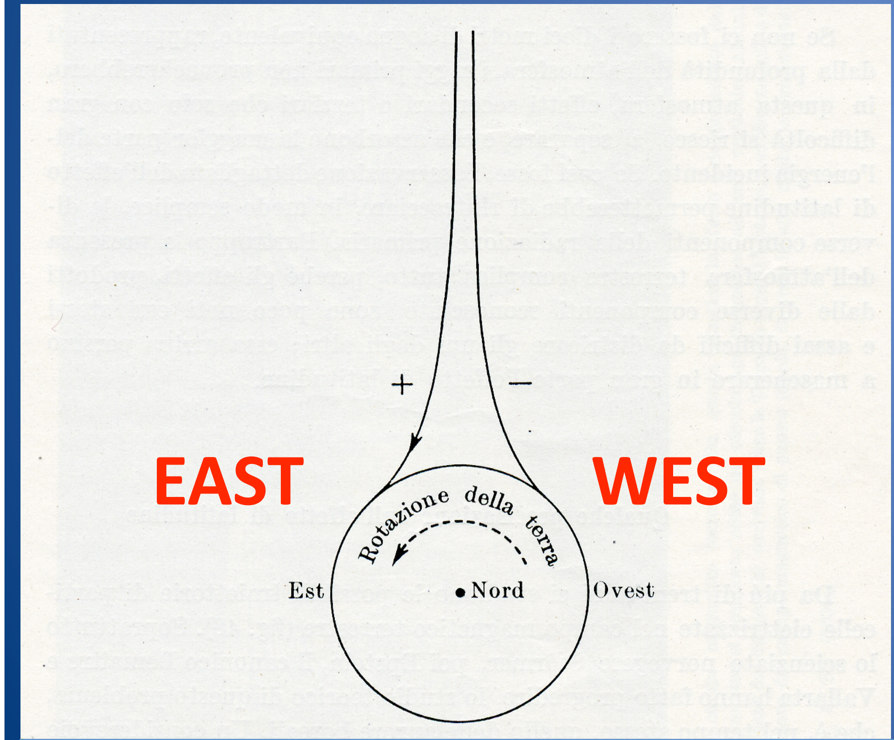

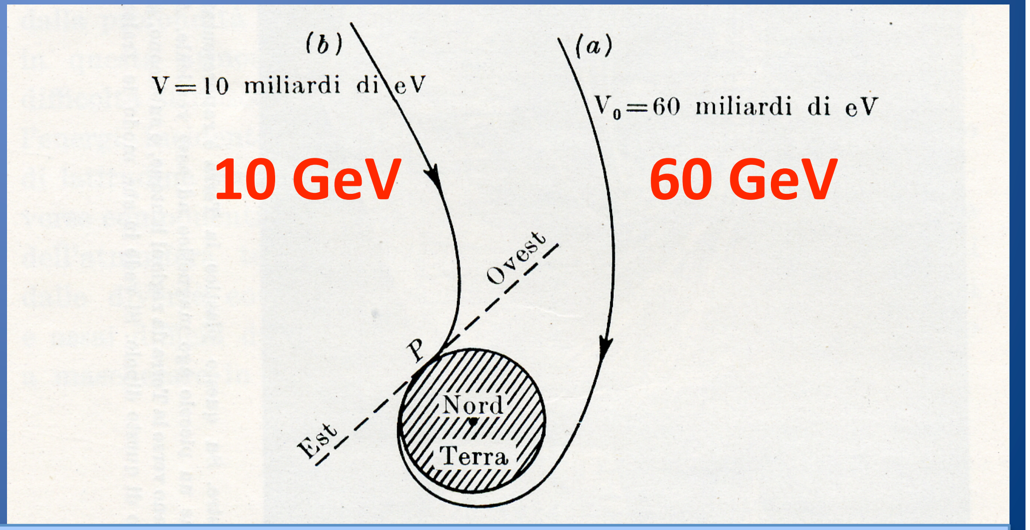

DIRECT Space “classical” energy/particle identification Experiment (E vs -dE/dx)

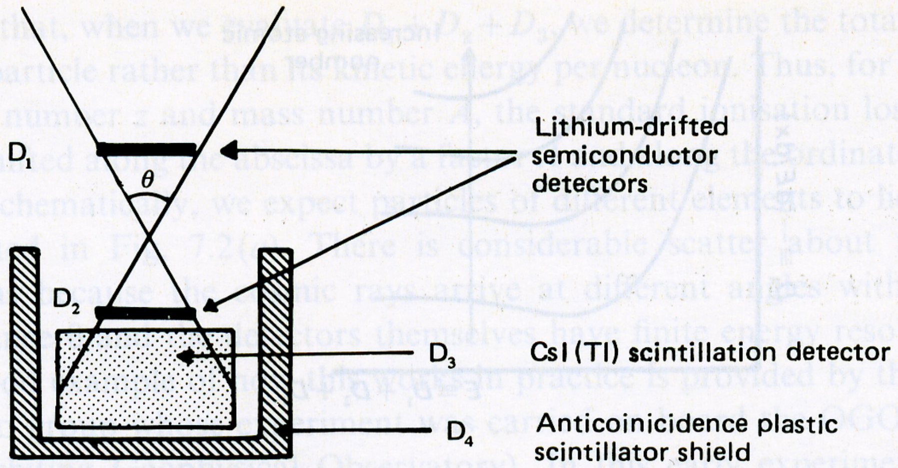

Figure 7.1. A simplified diagram showing the layout of the detectors of the cosmic ray telescope flown on board the IMP-III space probe. (From M. M. Shapiro and R. Silberberg (1970). *Ann. Rev. Nucl. Sci.*, **20**, 323.)

Space "classical" energy/particle identification Experiment (E vs -dE/dx)

Geometry
-dE/dx

Energy
Calorimetry

AC for
Containement

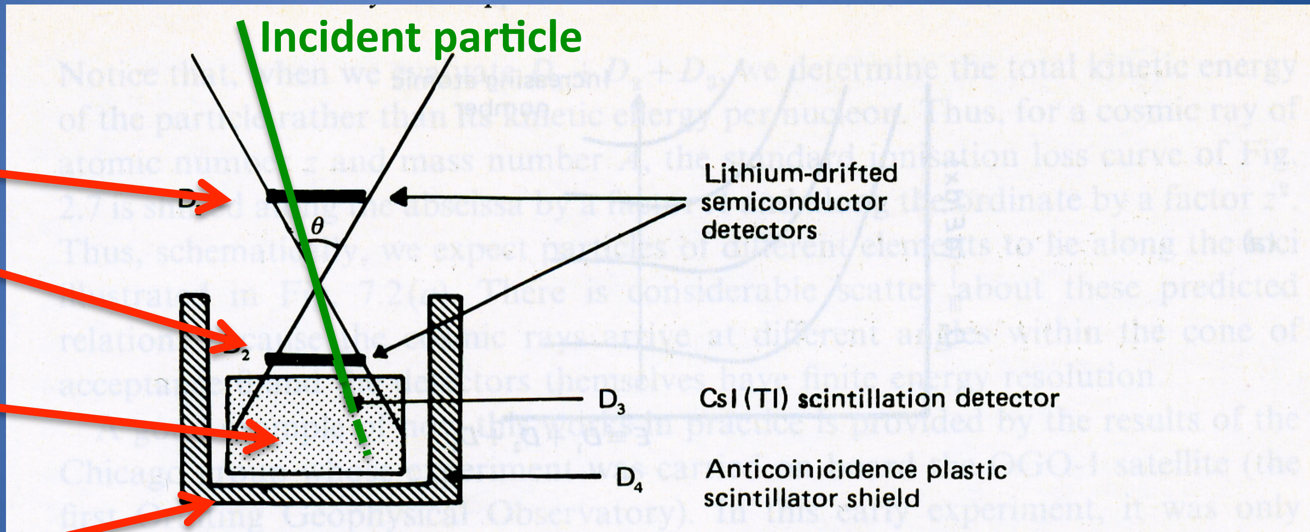

Figure 7.1. A simplified diagram showing the layout of the detectors of the cosmic ray telescope flown on board the IMP-III space probe. (From M. M. Shapiro and R. Silberberg (1970). *Ann. Rev. Nucl. Sci.*, **20**, 323.)

Passage of ch. particles through matter (I)

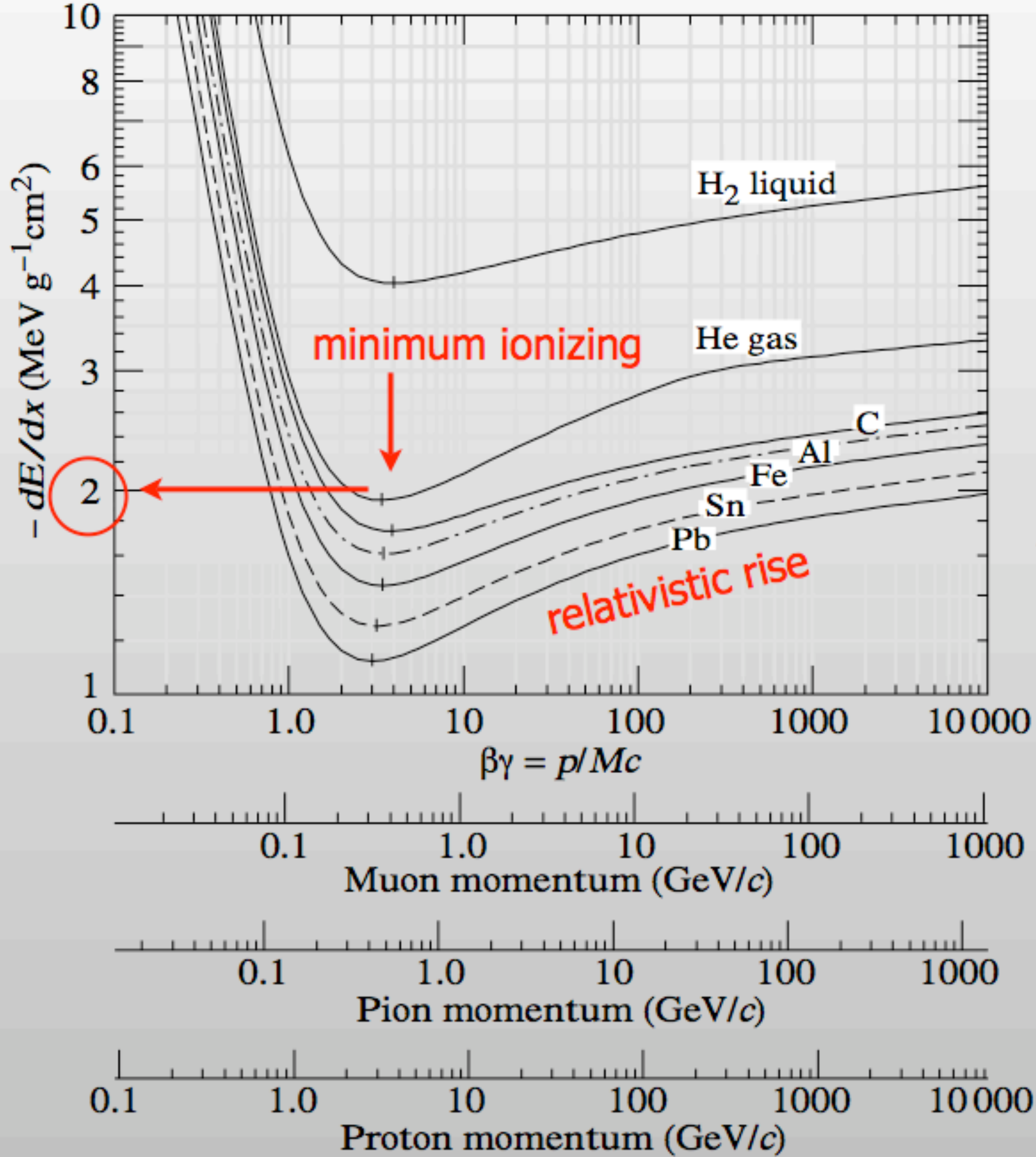

$(dE/dx)_{min} \approx$
2 MeV/(g cm^2)

A “calorimeter” light collection

$$I \sim n_{ph} \sim E_{loss} \sim E_o$$

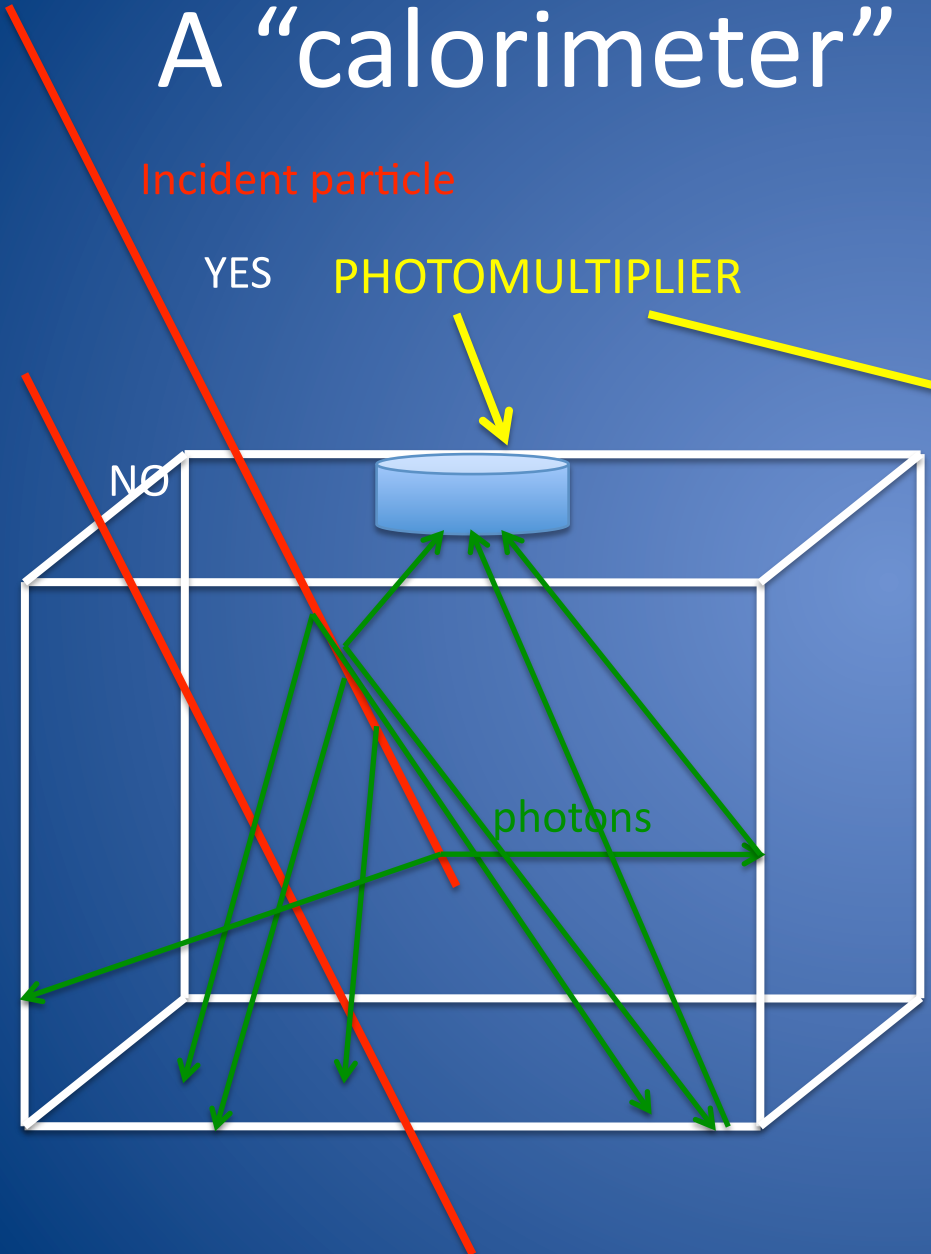

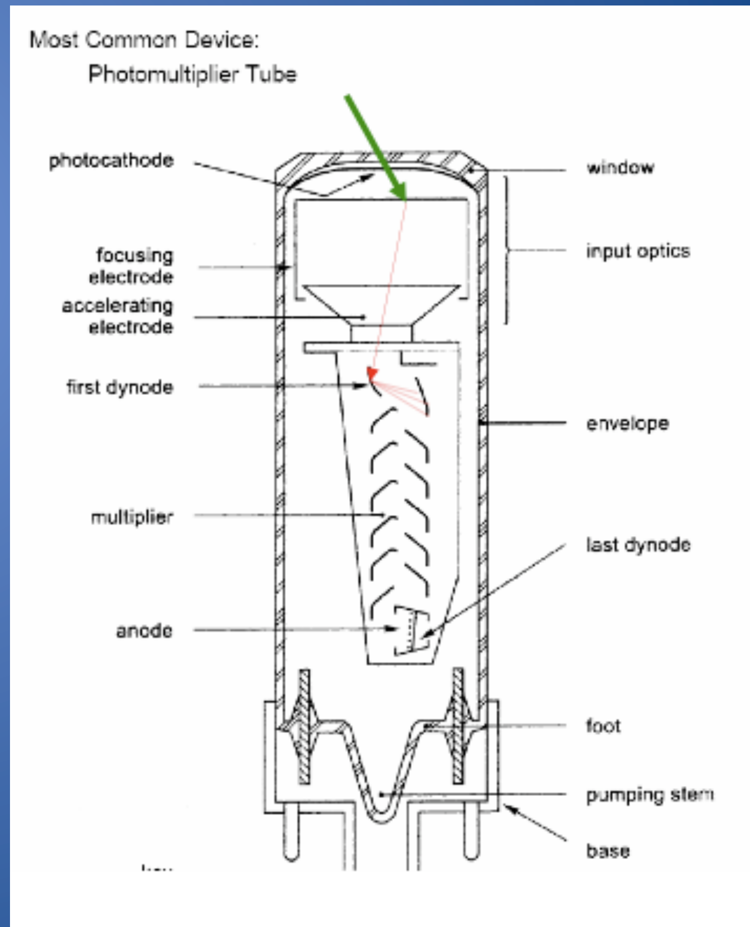

Calorimetry

Energy is converted into "quantum" (photons, pairs…
scintillator, semiconductors…)

n of quantum detected = $n_0 \cdot \varepsilon$

n_0 = quantum produced = Eo / Eq (Eq = energy necessary to produce a quantum: 100 eV, 1 eV…)

ε = quantum recording efficiency

Resolution dominated by statistical fluctuations:

$$\sigma(Eo) / Eo = \sqrt{n} / n = 1 / \sqrt{n} = \sqrt{Eq/\varepsilon\, Eo} = c / \sqrt{Eo}$$

$\sigma(Eo) / Eo$ about " 10 % /$\sqrt{Eo\ (MeV)}$ "

With scintillator and ε about 1 % (ε assumed including e.g. q.e.)

Energy losses of charged particles & space detectors

$$-\frac{dE}{dx} = Kz^2 \frac{Z}{A} \frac{1}{\beta^2} \left[\frac{1}{2} \ln \frac{2m_e c^2 \beta^2 \gamma^2 T_{max}}{I^2} - \beta^2 - \frac{\delta}{2} \right]$$

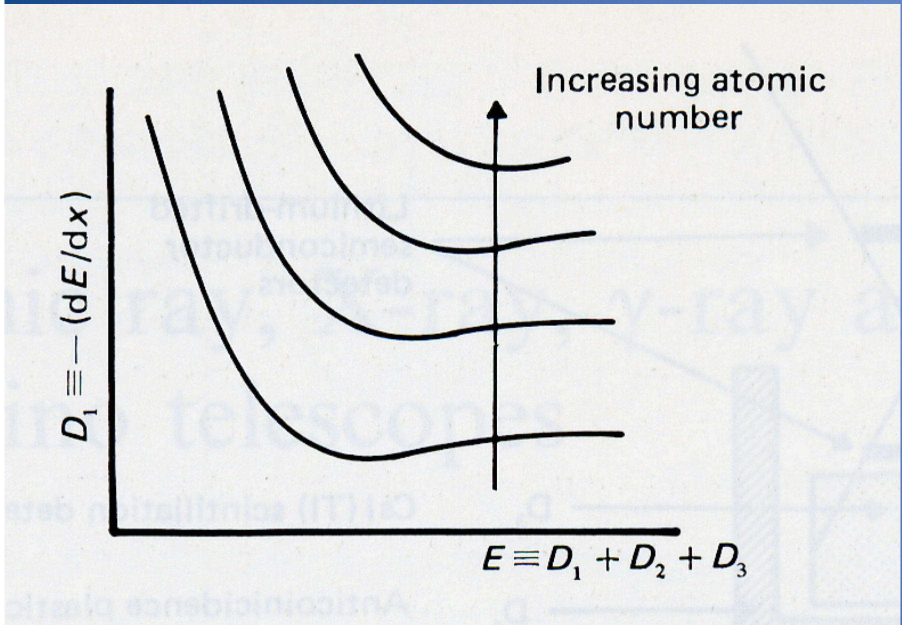

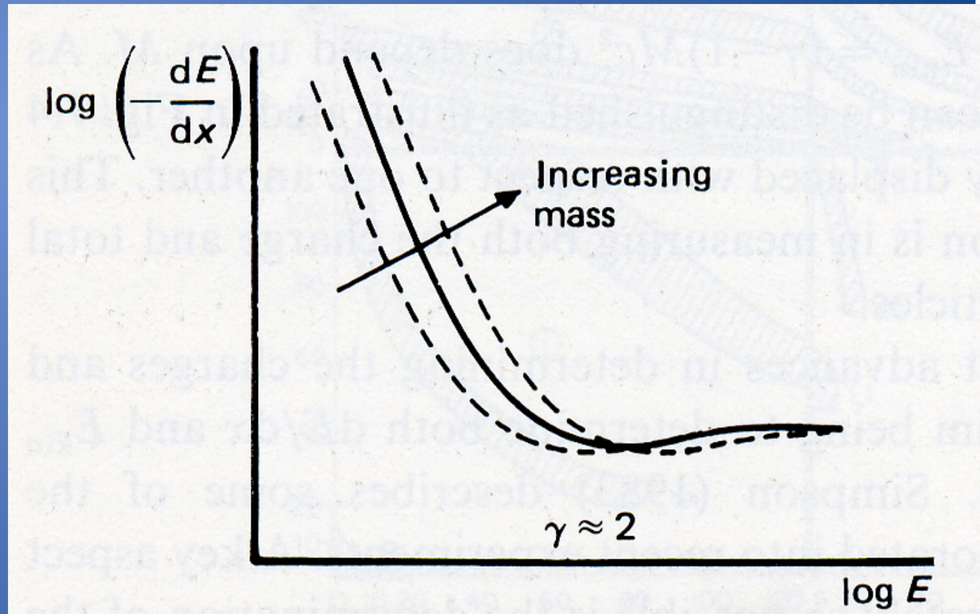

$1 / v^2 \approx M / E$

CRIS: Cosmic Ray Isotope Spectrometer

launched August '97

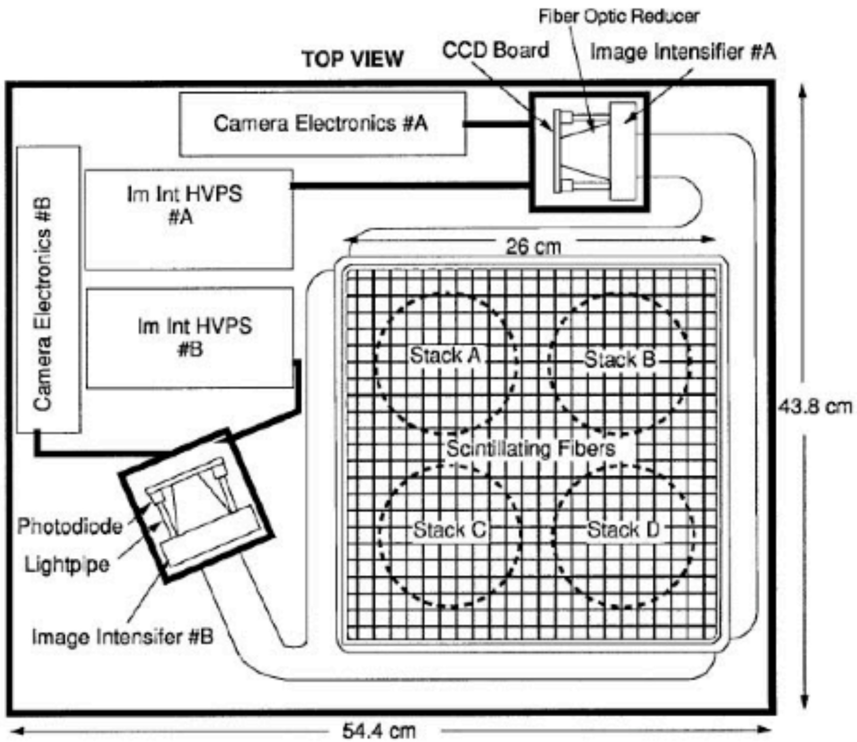

Bethe Bloch:

$$\Delta E \propto \frac{z^2 \cdot A}{E}$$

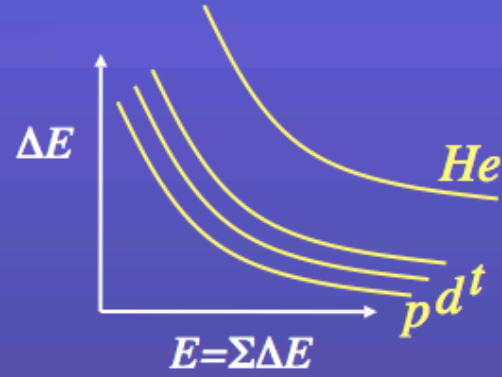

Multiple ΔE measurements in each particle track

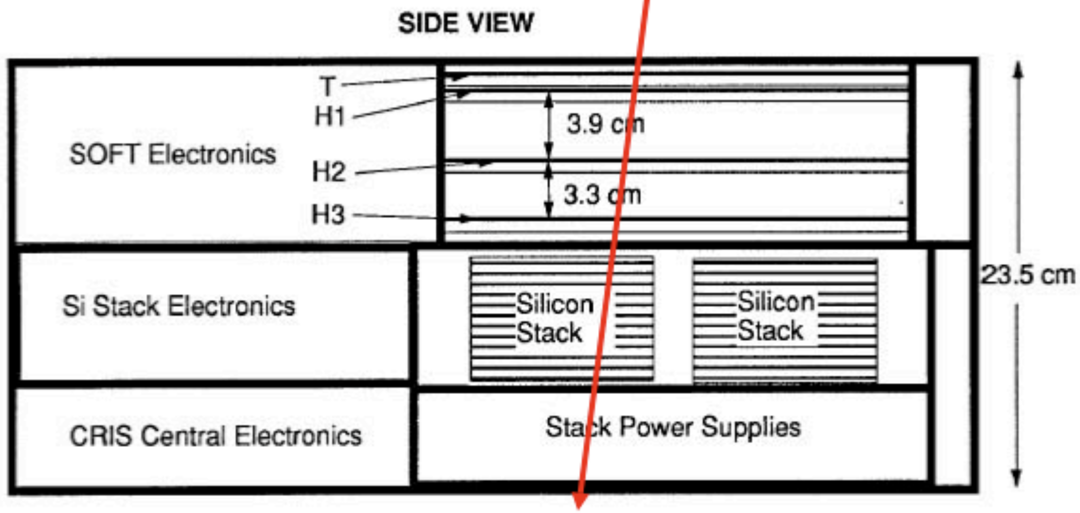

CRIS: Cosmic Ray Isotope Spectrometer

launched August '97

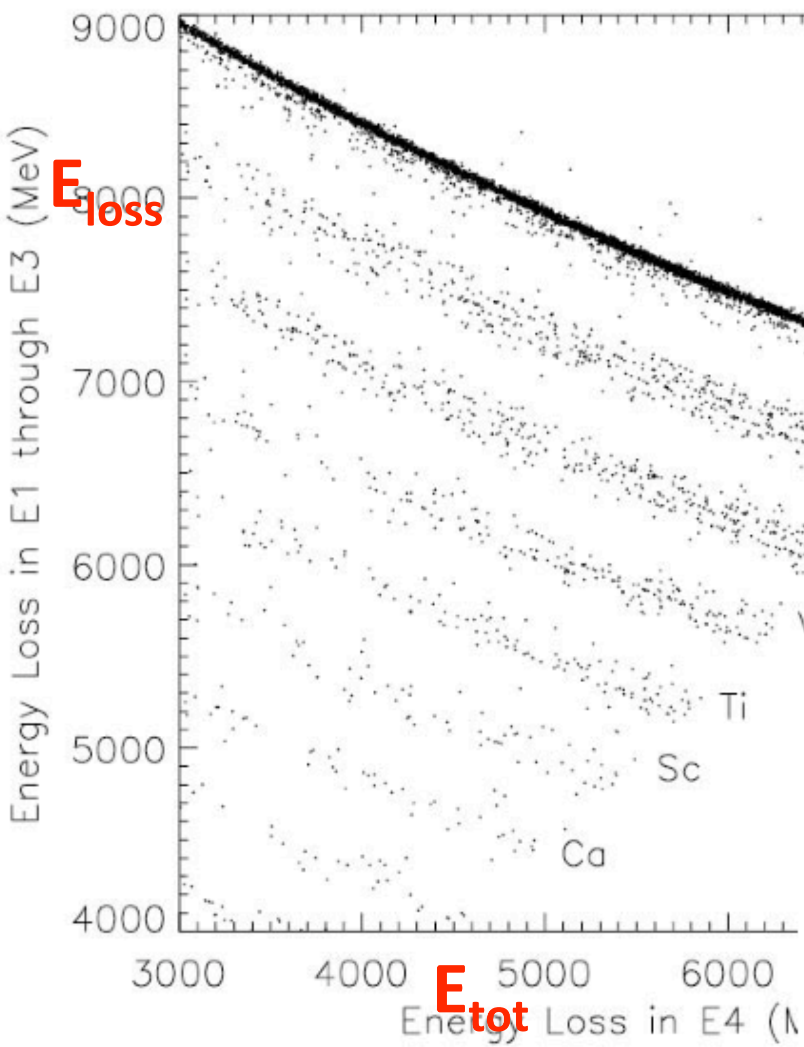

Bethe Bloch:

$$\Delta E \propto \frac{z^2 \cdot A}{E}$$

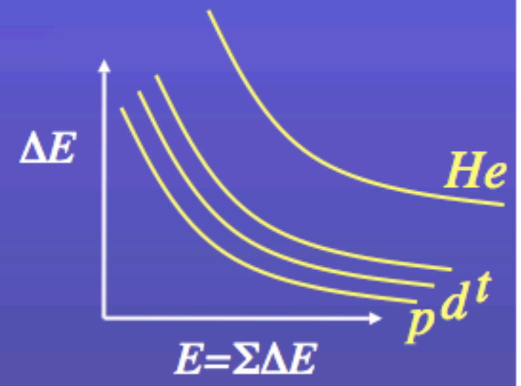

Multiple ΔE measurements in each particle track

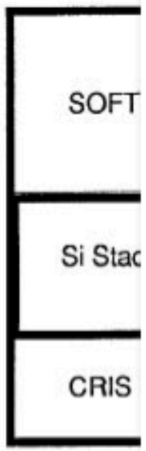

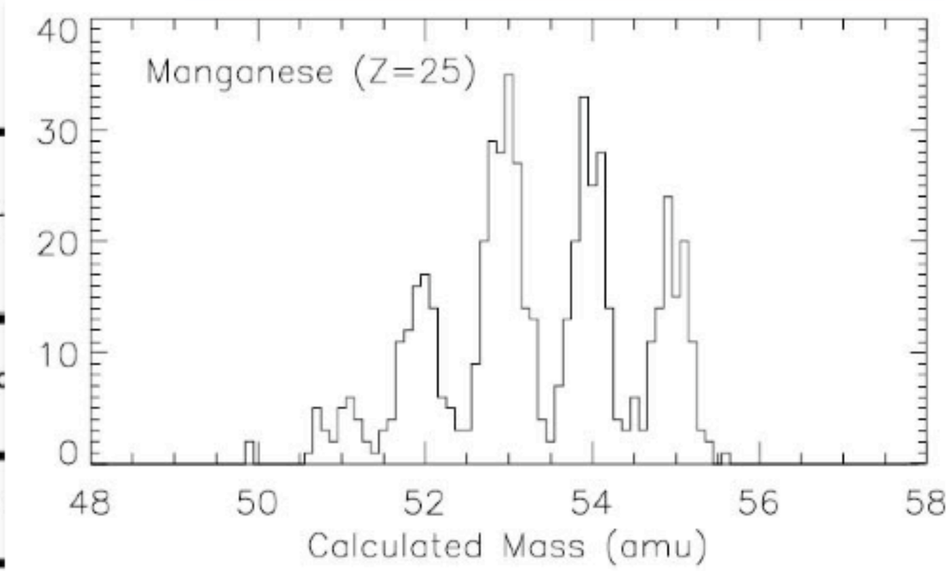

Cherenkov light

Qualitatively: polarization of the molecules of the medium due to the electric field of the incident particle. The depolarization composes destructively in all directions except, for ultra-relativistic particles, in direction θ_c (as for a shock wave from a supersonic aircraft)

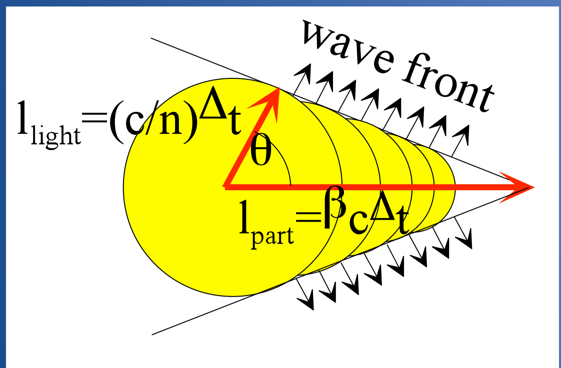

$$\boxed{\cos\theta_C = \frac{1}{n\beta}} \quad \text{with} \quad \underline{n = n(\lambda) \geq 1}$$

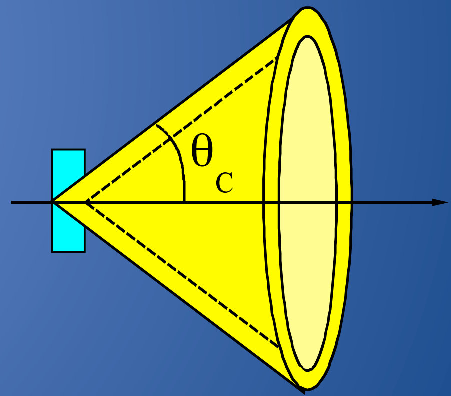

Threshold velocity: $\beta_s = 1/n \rightarrow \theta_c \sim 0$

Maximum angle: $\theta_{max} = \arccos(1/n)$

Cherenkov light

Number of photons emitted per path-length and wavelength unit.
It decreases with increasing λ.

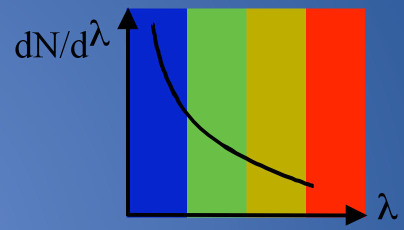

$$\frac{d^2N}{dxd\lambda} = \frac{2\pi z^2\alpha}{\lambda^2}\left(1-\frac{1}{\beta^2 n^2}\right) = \frac{2\pi z^2\alpha}{\lambda^2}\sin^2\theta_C$$

$$\frac{d^2N}{dxd\lambda} \propto \frac{1}{\lambda^2} \quad \text{with} \;\; \lambda = \frac{c}{\nu} = \frac{hc}{E} \qquad \frac{d^2N}{dxdE} = const.$$

Cherenkov light

$$\frac{d^2N}{dxd\lambda} = \frac{2\pi z^2\alpha}{\lambda^2}\left(1 - \frac{1}{\beta^2 n^2}\right) = \frac{2\pi z^2\alpha}{\lambda^2}\sin^2\theta_C$$

$$\frac{d^2N}{dxd\lambda} \propto \frac{1}{\lambda^2} \quad \text{with } \lambda = \frac{c}{\nu} = \frac{hc}{E} \quad \frac{d^2N}{dxdE} = const.$$

medium	n	θ_{max} (β=1)	N_{ph} (eV^{-1} cm^{-1})
air	1.000283	1.36	0.208
isobutane	1.00127	2.89	0.941
water	1.33	41.2	160.8
quartz	1.46	46.7	196.4

deg

ΔE =1 eV ~ $\Delta\lambda$ = 300 - 600 nm

Cherenkov light

- Energy measurement and particle identification
- Threshold
- Angle
- Particle identification:

  β + momentum (e.g. through a magnetic field)

  => mass

SUPER-KAMIOKANDE
CHERENKOV LIGHT MUON DECAY

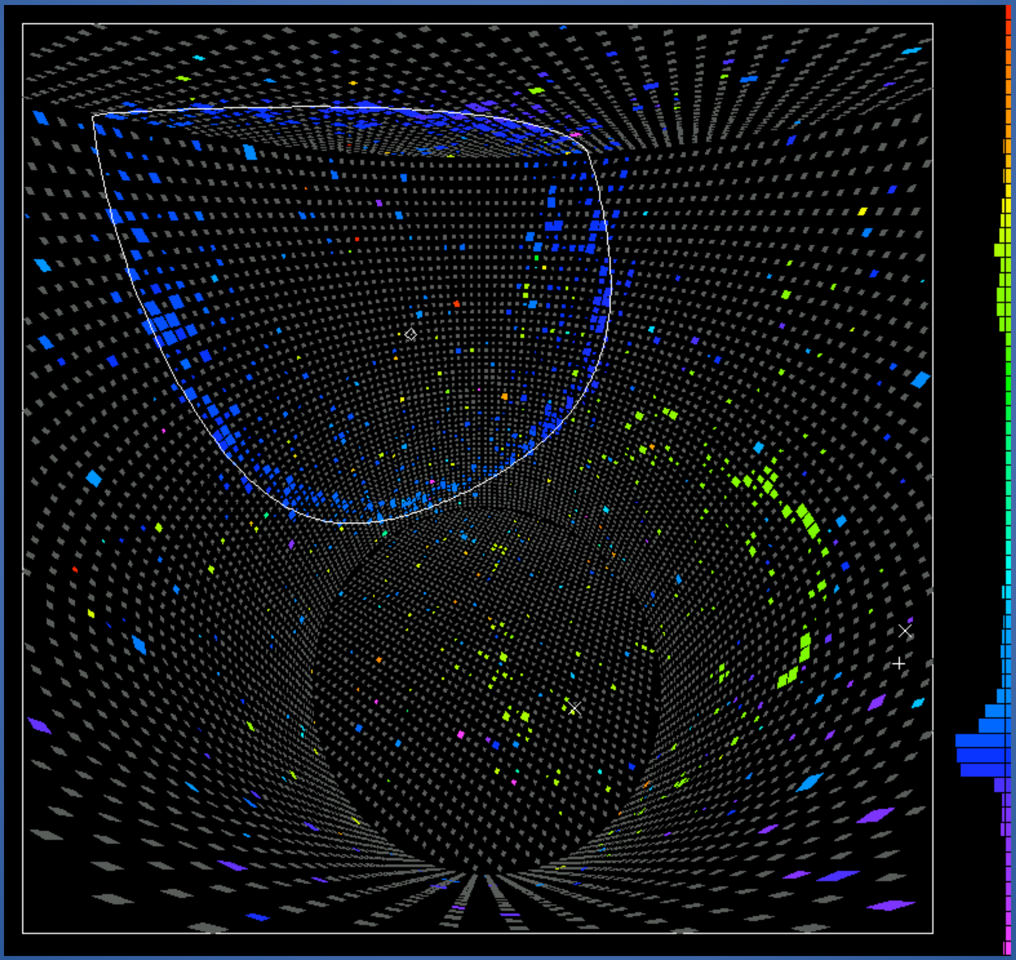

SUPER-KAMIOKANDE: huge underground water Cherenkov light detector

SUPER-KAMIOKANDE

CHERENKOV LIGHT E.M. SHOWER

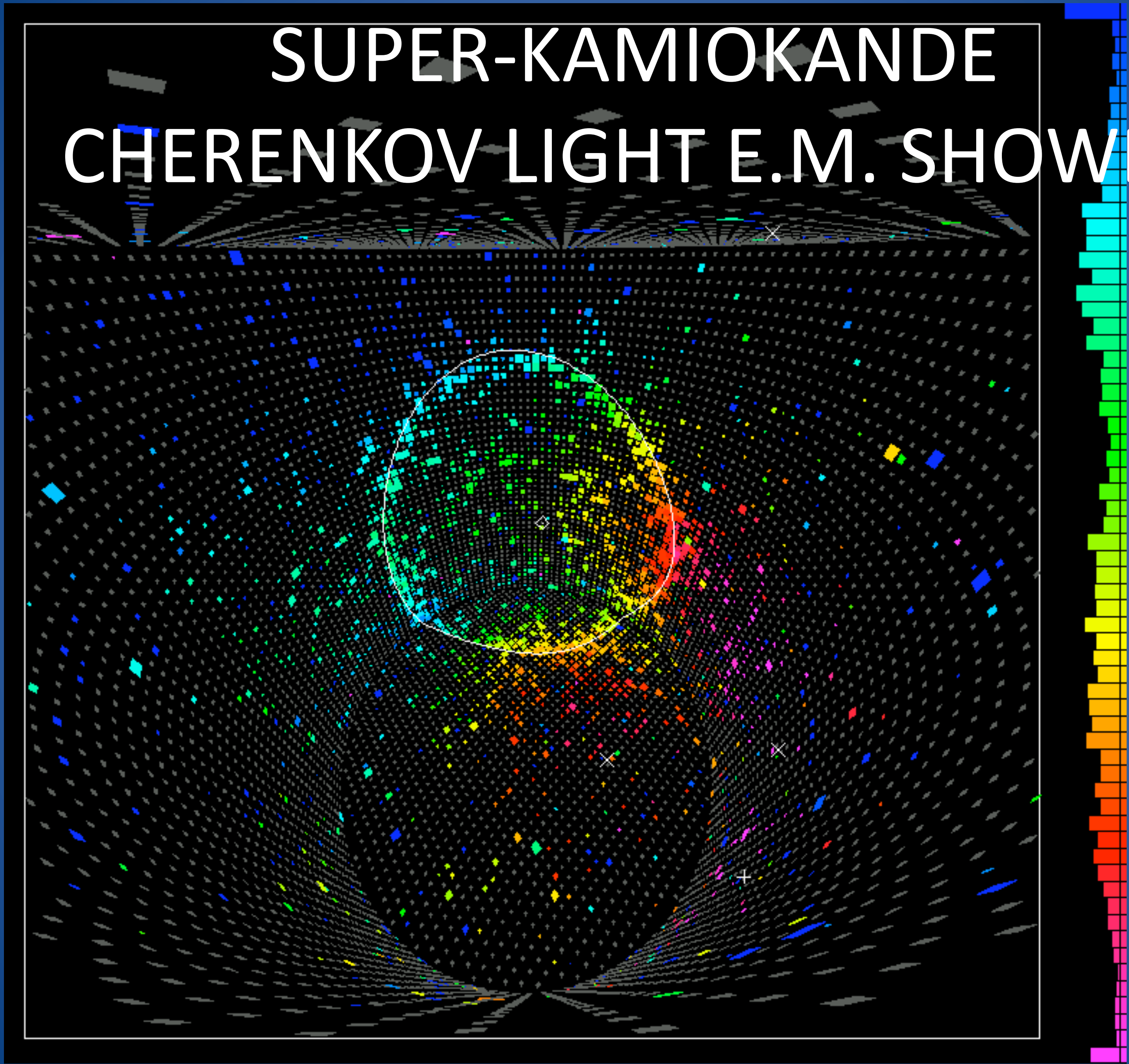

Cherenkov detectors HEAO-C3

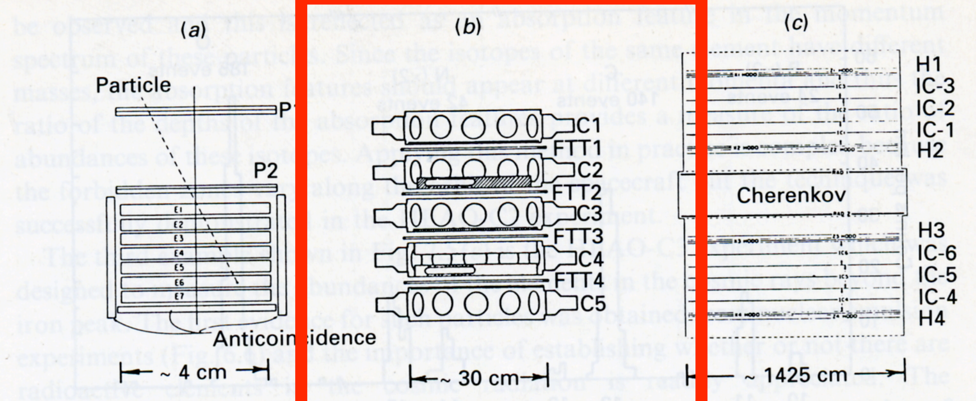

Figure 7.5. Examples of three important cosmic ray satellite telescopes. (From J. A. Simpson (1983). *Ann. Rev. Nucl. Part. Sci.*, **33**, 351.)
(*a*) A schematic diagram of an ISEE class telescope for the measurement of cosmic ray isotopes. (W. E. Althouse, A. C. Cummings, T. L. Garrard, R. A. Meawaldt, E. C. Stone and R. E. Vogt (1978). *IEEE Trans. Geosci. Electron.*, **GE15**, 204.)
(*b*) The HEAO-C2 experiment of the Danish–French collaboration. (Copenhagen–Saclay Collaboration (1981). *Adv. Space Res.*, **1**, 173.)
(*c*) The HEAO-C3 ultraheavy nuclei telescope for the study of cosmic rays with $Z \geqslant 30$. (W. R. Binns, M. H. Israel, J. Klarmann, W. R. Scarlett, E. C. Stone and C. J. Waddington (1981). *Nucl. Instrum. Methods*, **185**, 415.)

n = 1.015 Eth = 4.5 GeV/nucl

1.33 0.5

isotopes identification through arrival directions and selection of forbidden zones in the Earth magnetic field

Atmosphere as a magnetic analyzer

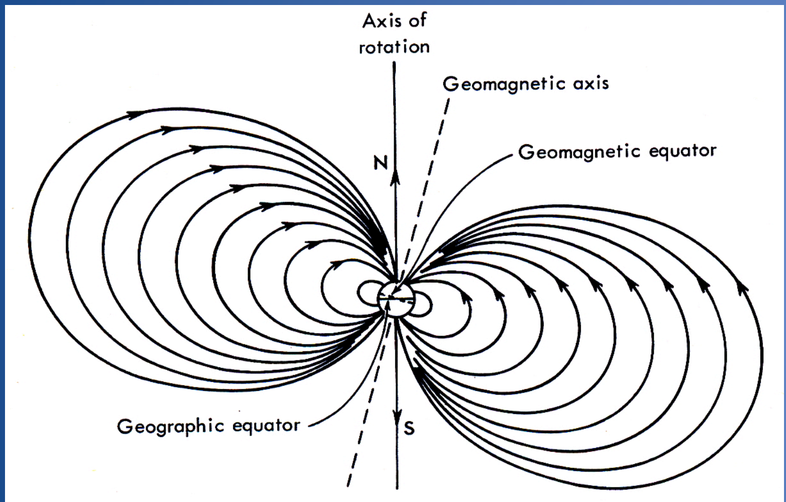

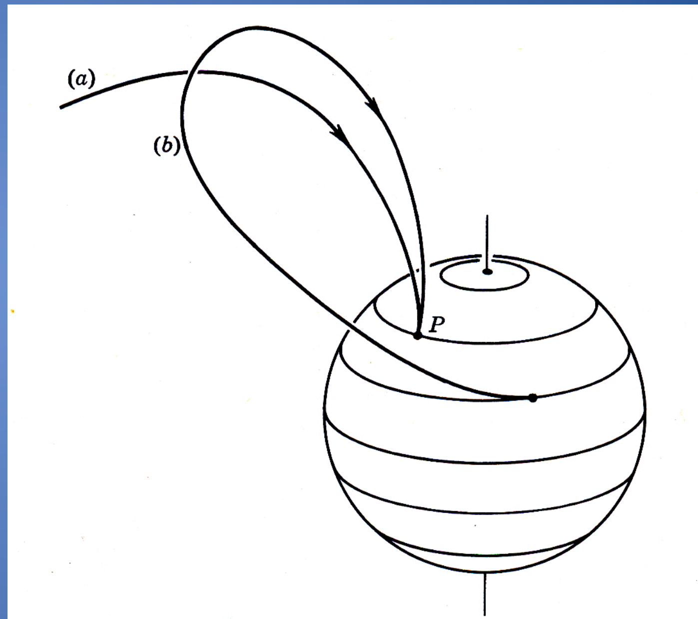

γ_E **= 300 (Z_e/M_{eV}) B Rc [gauss cm]**

Allowed and forbidden directions given γ (measured by CL) depend on M

HEAT-pbar (High Energy Antimatter Telescope)

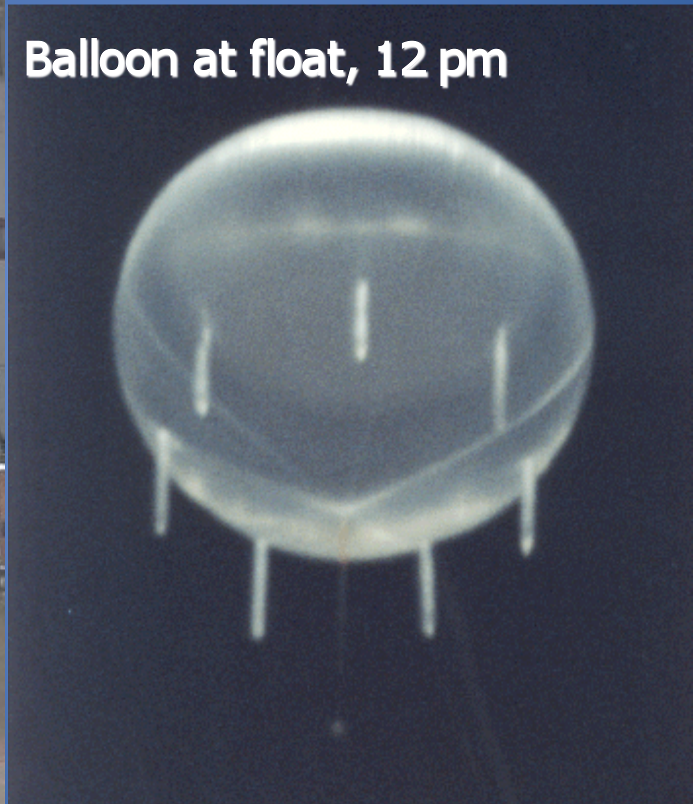

Superconducting Magnet Spectrometer with Drift Tube Hodoscope (DTH), Multiple Ionization (dE/dx) Detector and Time-of-Flight (TOF) system.

Identifying Antiprotons with HEAT-pbar

- DTH:
  - p from amount of bending in B=1T
  - Sign of Z from direction

R=pc/Ze,
Rmax = 170 GV

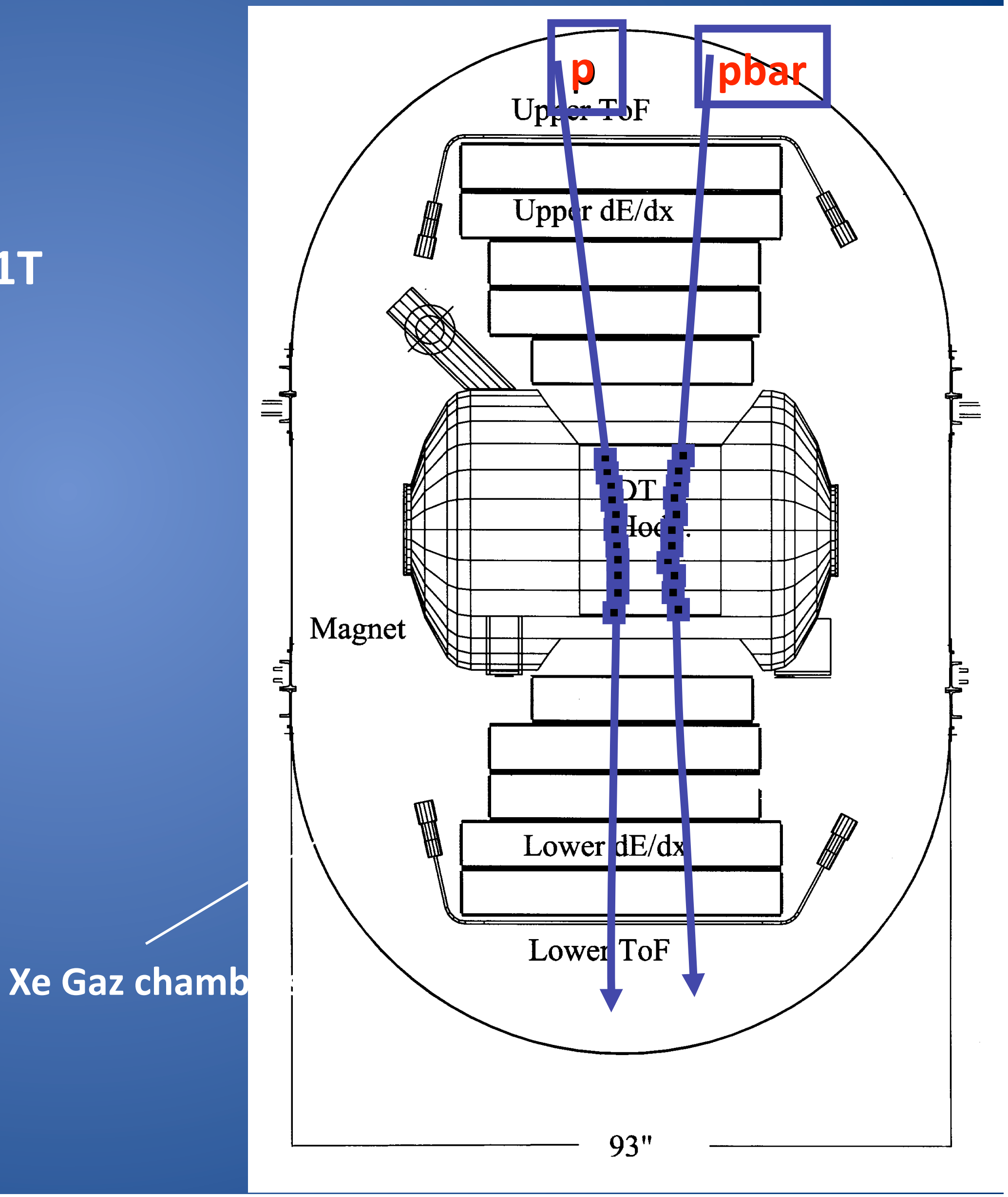

Identifying Antiprotons with HEAT-pbar

Up going proton (albedo particles) looks like down going antiproton -> Need to know start and stop in the ***time-of-flight***

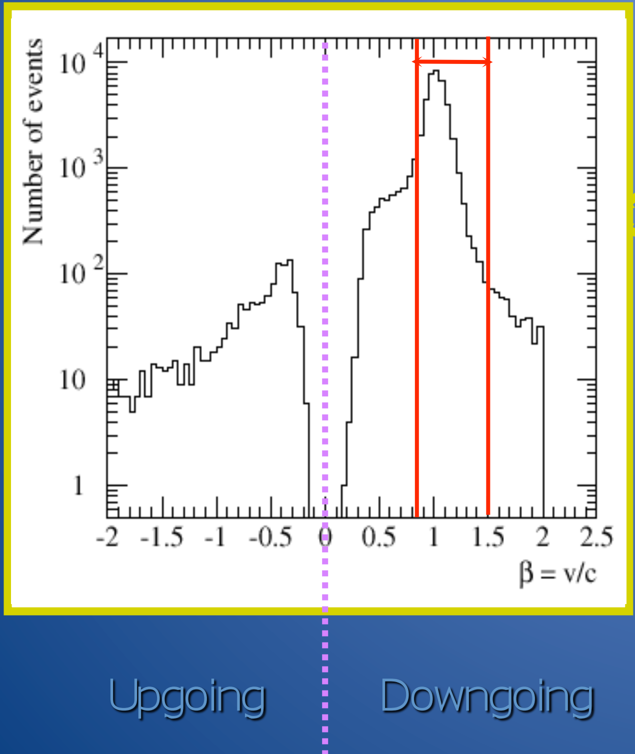

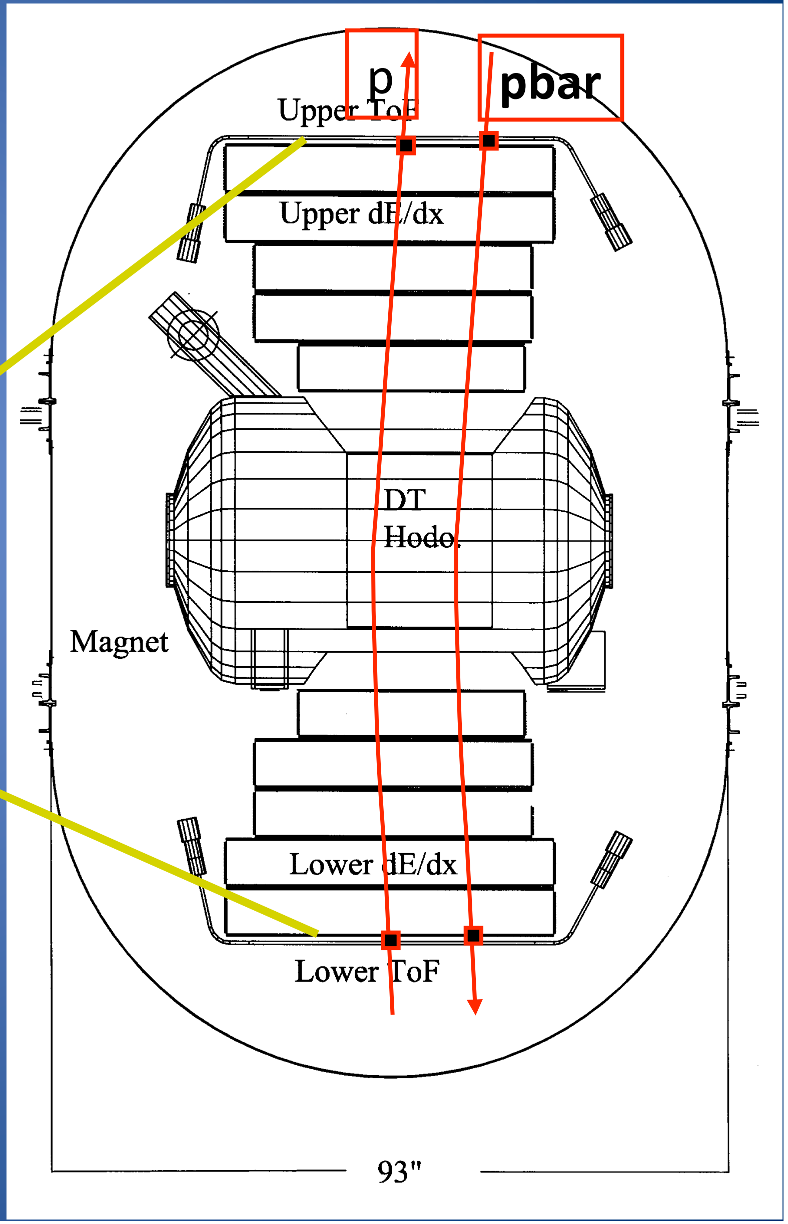

New major project: PAMELA

Pamela (launched 15.5.06)

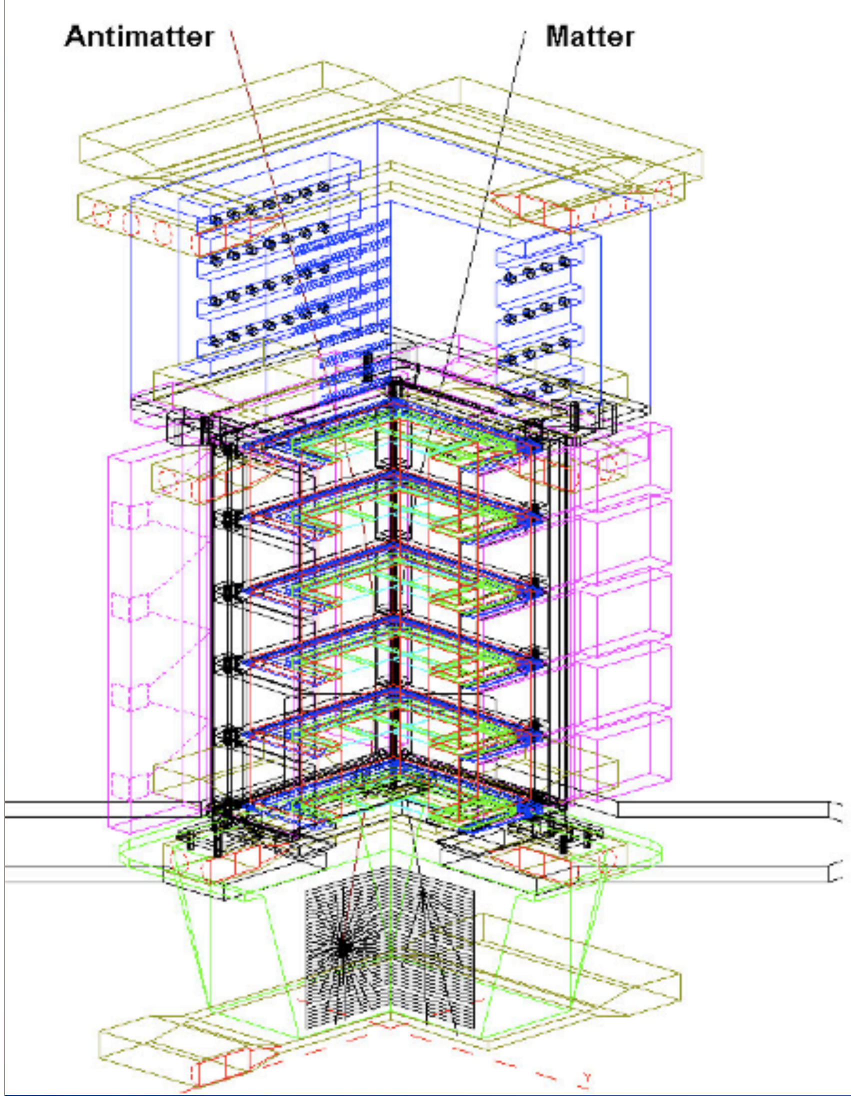

on-board of the Russian
Resurs-DK1 satellite by Sojuz rocket

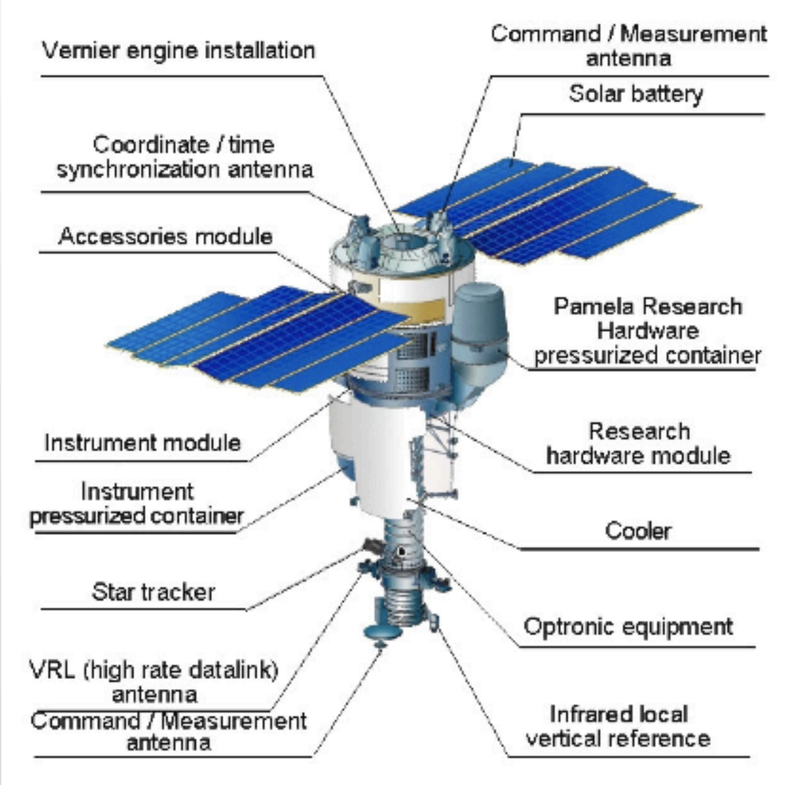

magnetic spectrometer with permament
0.4 T magnet, calorimeter, ToF, TRD, ...
size: 120 x 40 x 45 cm^3; weight: 380 kg

PAMELA launch

15.5.2006, Baikonur Cosmodrome Kazakhstan

The cloud chamber (1929)

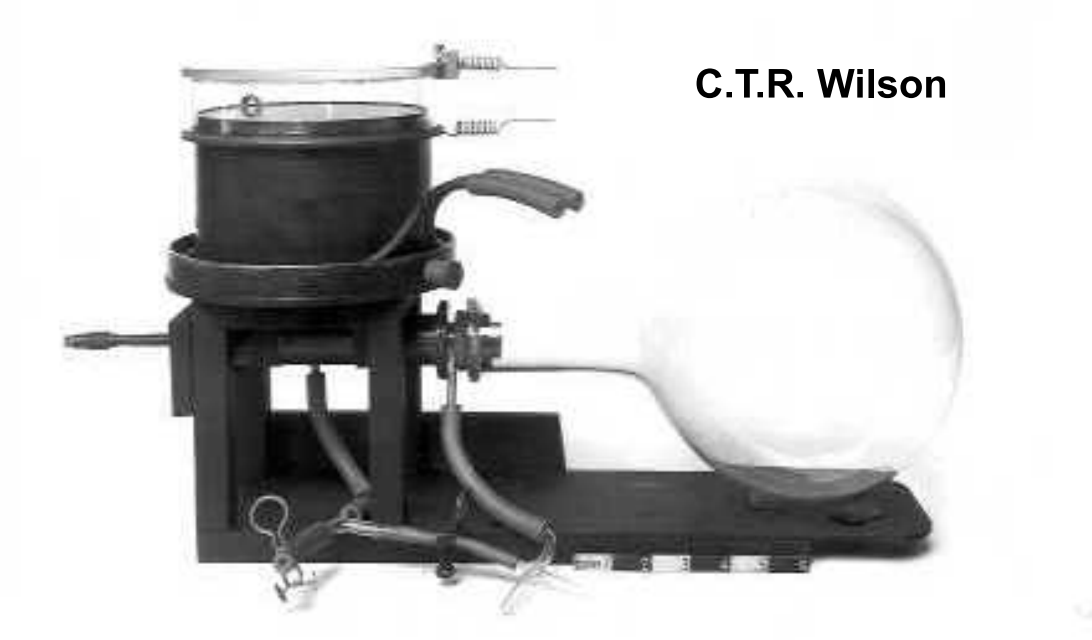

Controlled by external trigger

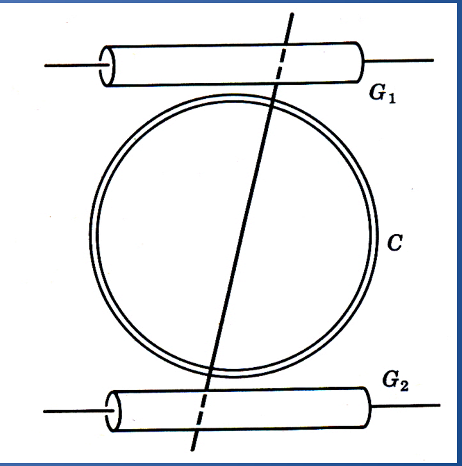

Fast expansion of gas in order to decrease temperature and over saturate the gas
Condensation of drops on the ions produced by particles

Blacket Occhialini (1931 - 1934)

E.M. SHOWERS

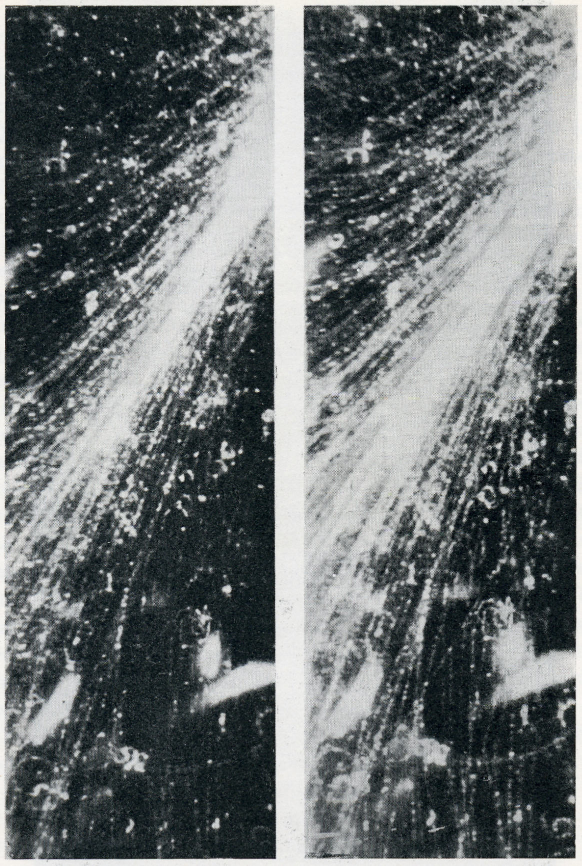

Fig. 45. Grande sciame di elettroni fotografato al laboratorio di Largentière con una camera di 80 cm di altezza e un campo magnetico di 3500 gauss. Vi si vedono un gran numero di elettroni, tanto positivi che negativi, di grande energia: nella parte inferiore della foto si vedono traiettorie circolari di elettroni, secondari di fotoni, prodotti anch'essi nello sciame.

LHERITIER, PEYROU, LAGARRIGUE, laboratorio di Largentière La Bessée (Delfinato).

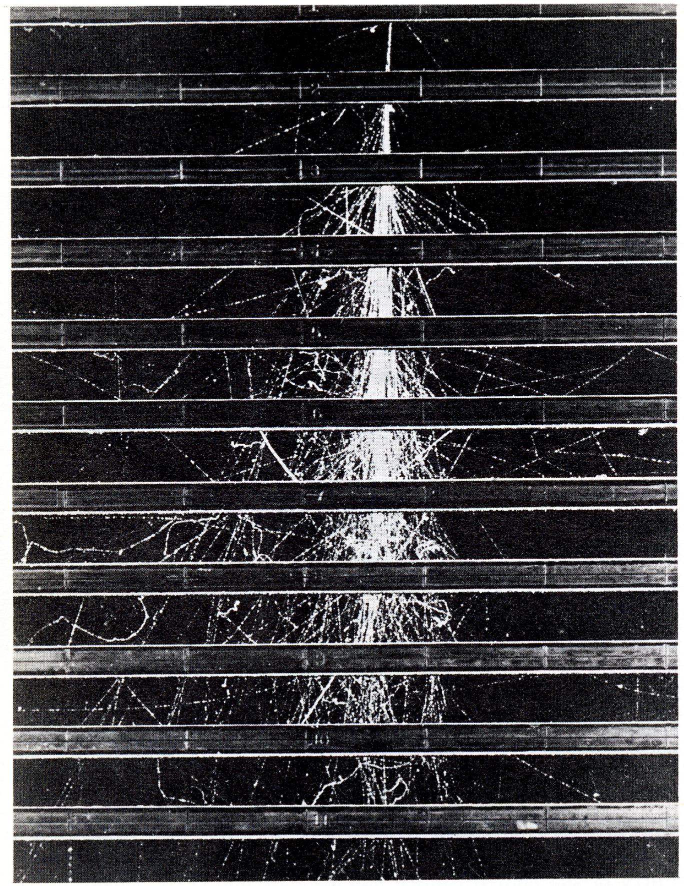

Fig. 7-5 A shower developing through a number of brass plates 1.25 cm thick placed across a cloud chamber. The shower was initiated in the top plate by an incident high-energy electron or photon. The photograph was taken by the MIT cosmic-ray group.

CALORIMETRY AT HIGH ENERGIES:
E.M. CASCADES

$N(t) = 2^t$

$\underline{E}\,(t) = E_0 / N(t) = E_0 / 2^t$

up to $\underline{E}(t) > E_{crit}$

for $\underline{E}(t) < E_{crit}$

$\rightarrow$ $-(dE/dx)_{coll}$ $\rightarrow$ absorption

$\underline{E}(t) = E_{crit}$ $\rightarrow$ $N(t)$ MAX

$E_{crit} = E_0 / 2^{tmax}$ $\quad$ $2^{tmax} = E_0 / E_{crit}$

$tmax = \ln (E_0/E_{crit}) / \ln 2$

$N(t)$ MAX $= N\,(tmax) = E_0 / E_{crit}$

$p\,(N) + A \rightarrow \pi^+ + \pi^- + \pi^0 + \ldots\ldots$

π^+ , π^- decay, interact

$\pi^0 \rightarrow \gamma + \gamma$

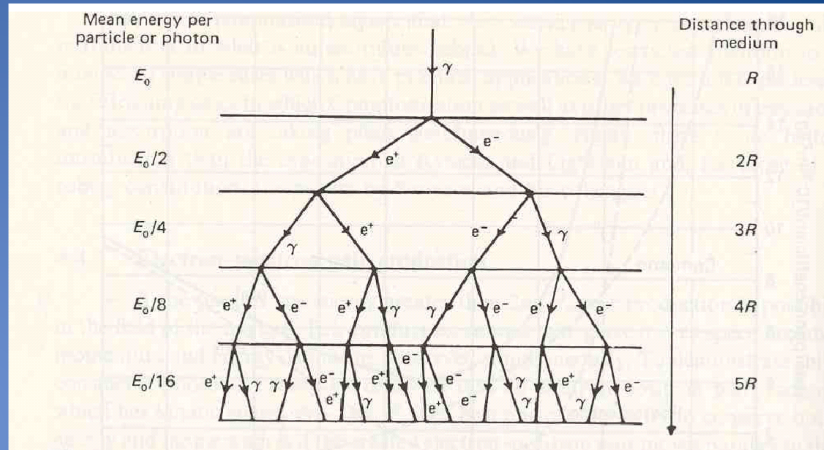

Figure 4.17. A simple model for an electromagnetic shower.

1 c.u. in carbon ~ 15 cm

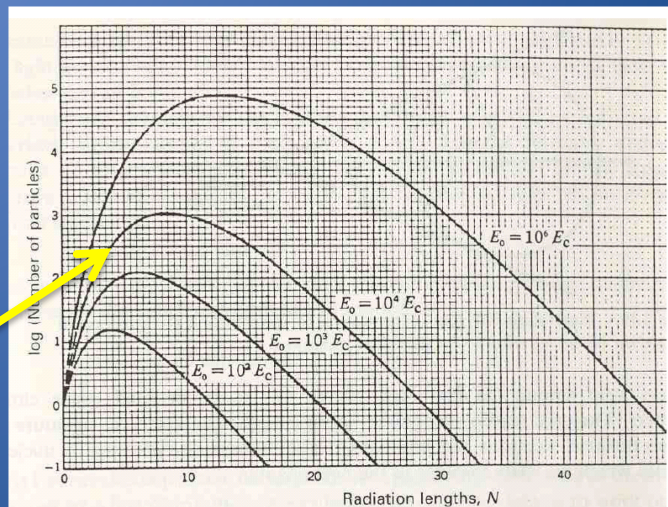

MEASUREMENT OF INTEGRAL BELOW THE RELATIVE CURVE

WHEN ENERGY CANNOT BE CONTAINED: SAMPLING CALORIMETERS

$\Delta E \sim$ Xsens/Xtot

~ 10 / 500 ~ 2 %

sens:

1 l r ~ 15 cm

ρ ~ 1 gr cm^{-3}

Ec ~ 80 MeV

abs:

1 l r ~ 1.8 cm

ρ ~ 7.8 gr cm^{-3}

Ec ~ 20.7 MeV

Sensitive material

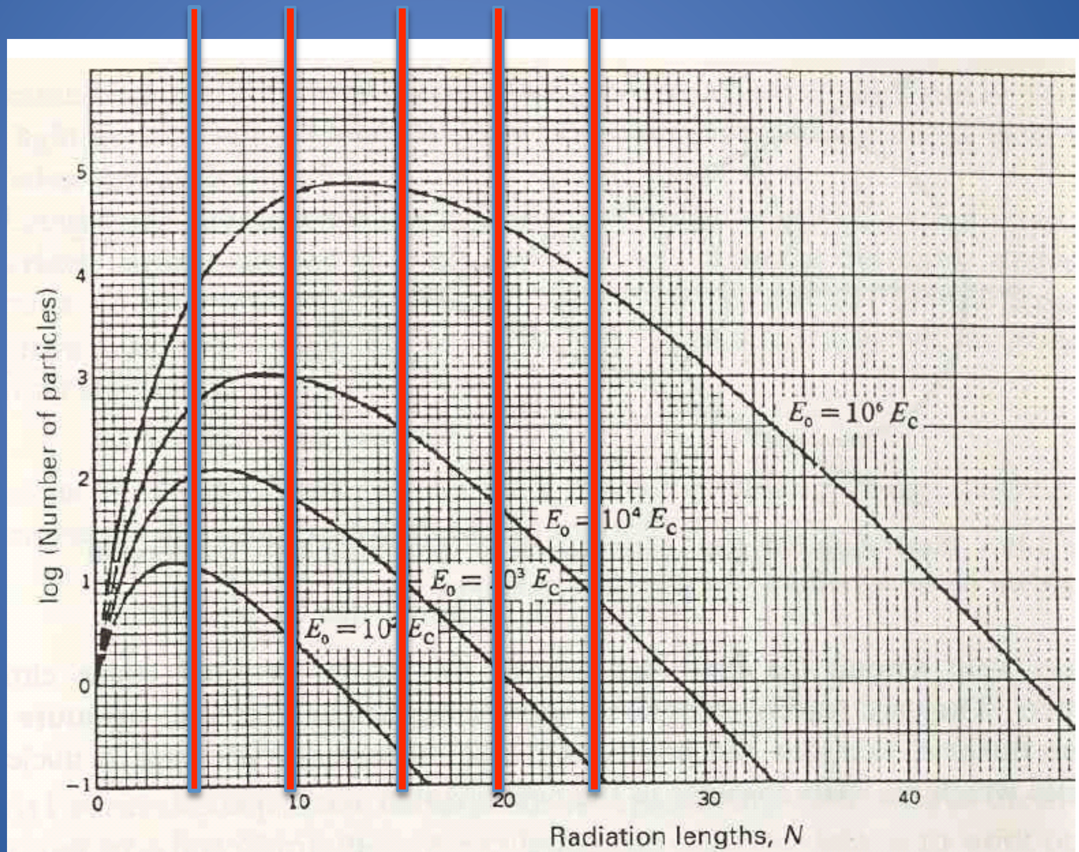

absorber

Sampling Calorimeters
Grigorov PROTON satellites

Fe 5 cm
Scint. 1.5 cm

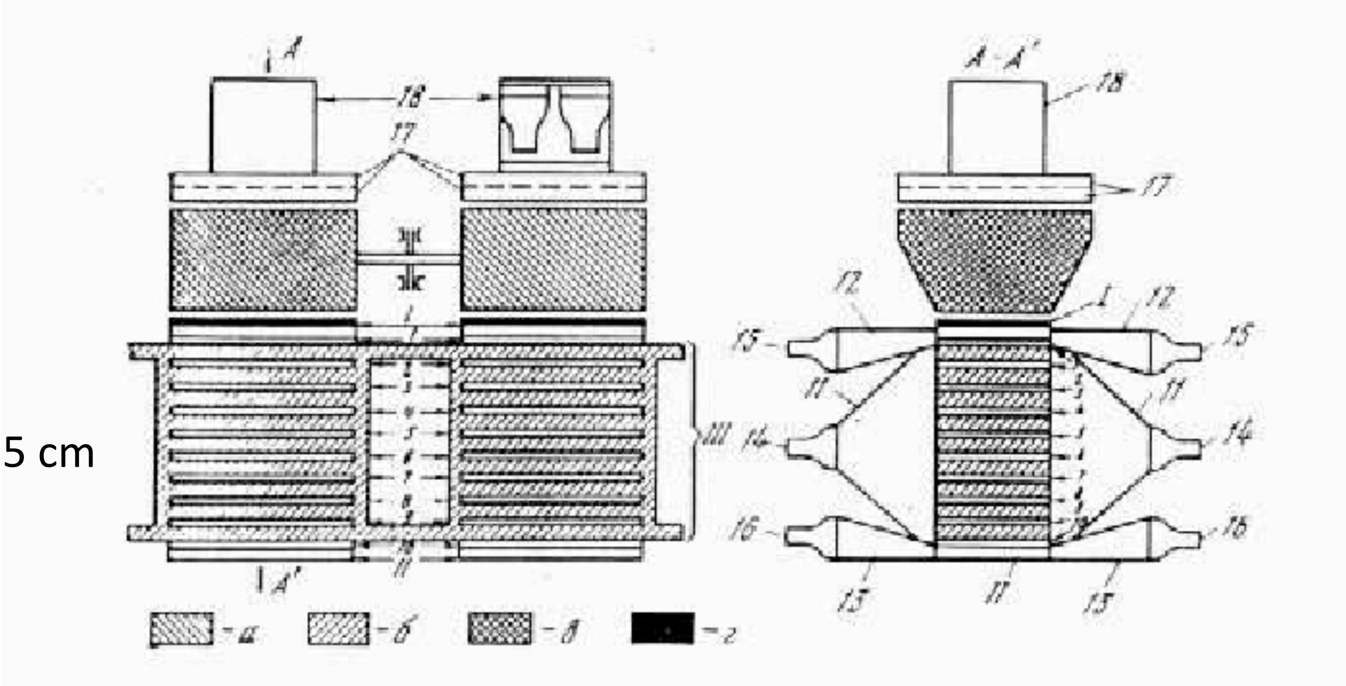

Рис. 9.1 Схематическое изображение прибора СЭЗ-14 I - детектор взаимодействия; II - нижний сцинтилляционный счетчик; III - ионизационный калориметр; 1-10 - сцинцилляционные детекторы энергии; 11 - диффузор детектора энергии; 12 - диффузор детектора взаимодействия; 14-16 - фотоумножители; 17 - детектор заряда (сдвоенный пропорциональный счетчик); 18 - детектор направления; а - полиэтилен; б - железо; в - углерод; г - свинец.

PROTON satellite calorimeter

Telescope:

$A = 1369\ cm^2$

Cerenkov counters (plexiglas):

Direction + charge

Calorimeter depth (Fe) 386 g/cm^2

$X \sim 2.7\ \lambda_{Fe}$

50% energy released

$E_o = 3.9 \cdot E_r$ (E_{th} = 29 GeV)

$\Delta E/E \sim 20$ % (my estimate)

Fraction of energy released inside the calorimeter

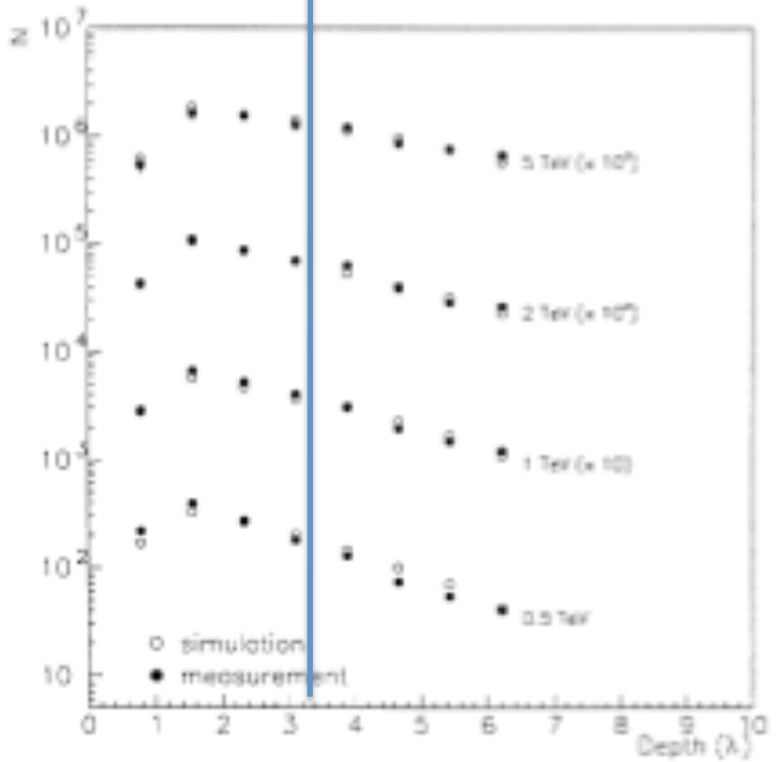

Fig. 11. Mean longitudinal transition curves for hadrons. Full circles: data; empty circles: simulation.

Hadron sampling calorimeters: resolutions

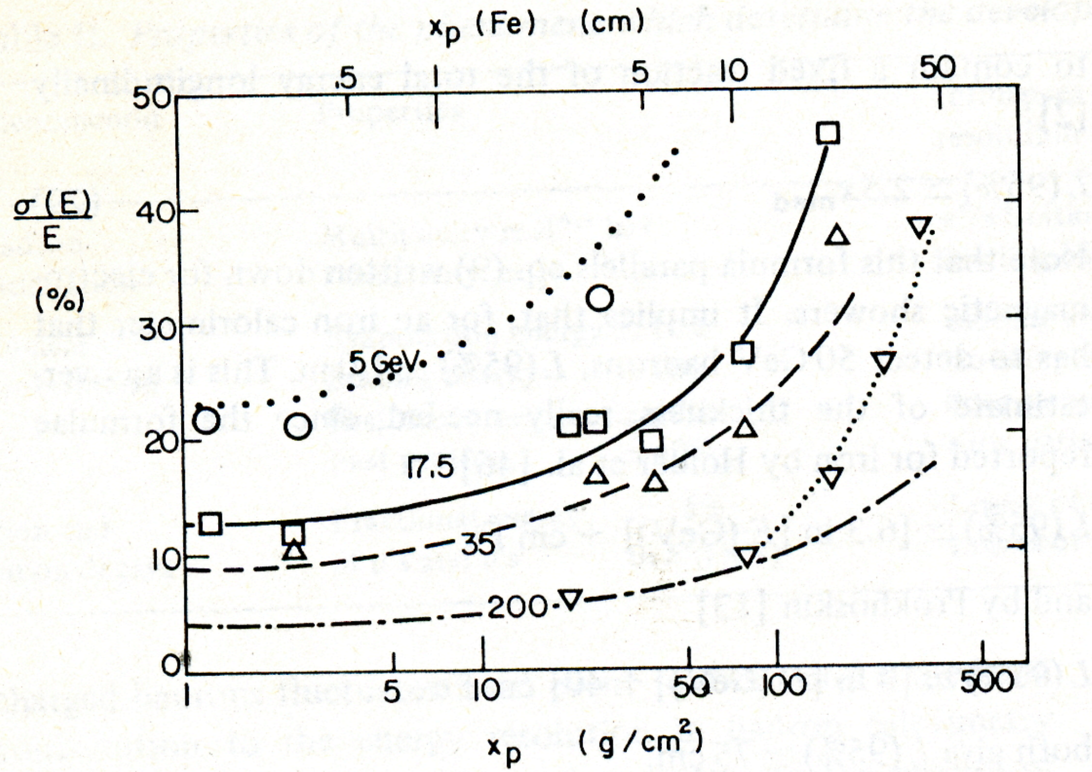

Fig. 19. The compilation by Iwata [2] on the thickness dependence of measured hadronic resolutions at 5, 17.5, 35 and 200 GeV is compared with the predictions of eq. (31) with $R' = 40\%$. The agreement is good below $\sim 100\,\mathrm{g\,cm^{-2}}$. The dotted curve above $100\,\mathrm{g\,cm^{-2}}$ is only meant to guide the eye through the 200 GeV points.


EMULSION CHAMBERS ON BALLOONS
JACEE
RUNJOB

Nuclear Emulsions

high energy
hadonic interaction
production of secondaries
fragmentation regions

==> elementary particle and high energy physics

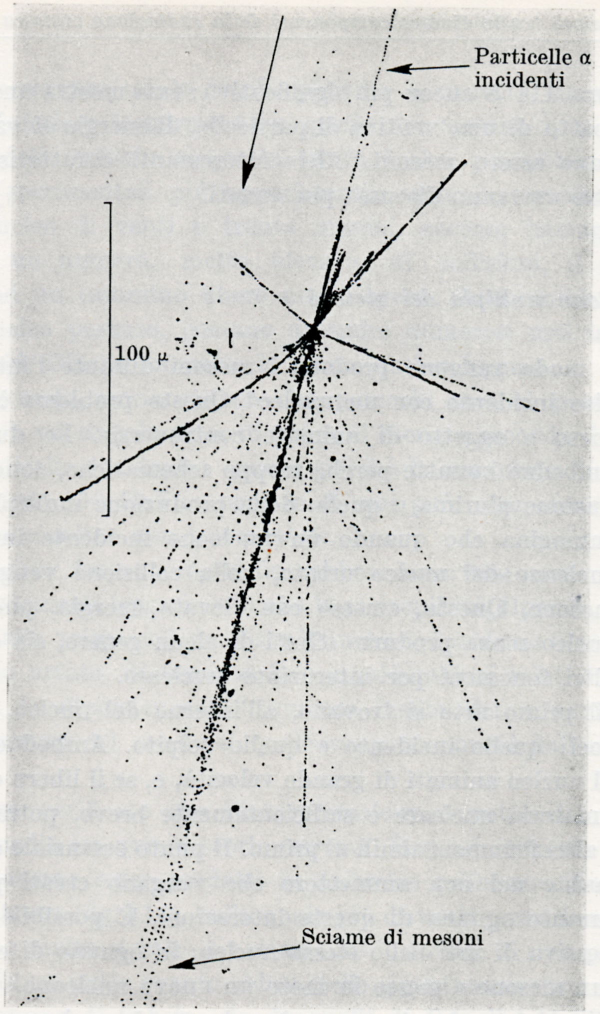

Fig. 114. Ecco uno dei fenomeni nucleari piú straordinari osservati fino ad ora. Una particella α dotata di energia superiore a 1000 GeV produce uno sciame formato da due gruppi di particelle relativistiche: il primo di 33 particelle piú allargato, e il secondo, di 23, emesso in un cono di piccolissima apertura. Le particelle di questo gruppo sono cosí collimate che non è possibile distinguerne le traiettorie nell'immediata vicinanza della stella. A una certa distanza dal centro di questa si osservano delle coppie di elettroni all'interno del cono di emissione: si tratta di coppie prodotte dai fotoni di disintegrazione dei mesoni neutri emessi insieme a quelli carichi nello sciame collimato.

KAPLON, PETERS e BRADT, « Phys. Rev. », 76, 1735 (1949).

Emulsions at high Altitude

Mt. Chacaltaya Bolivia

5200 m (540 g/cm^2)

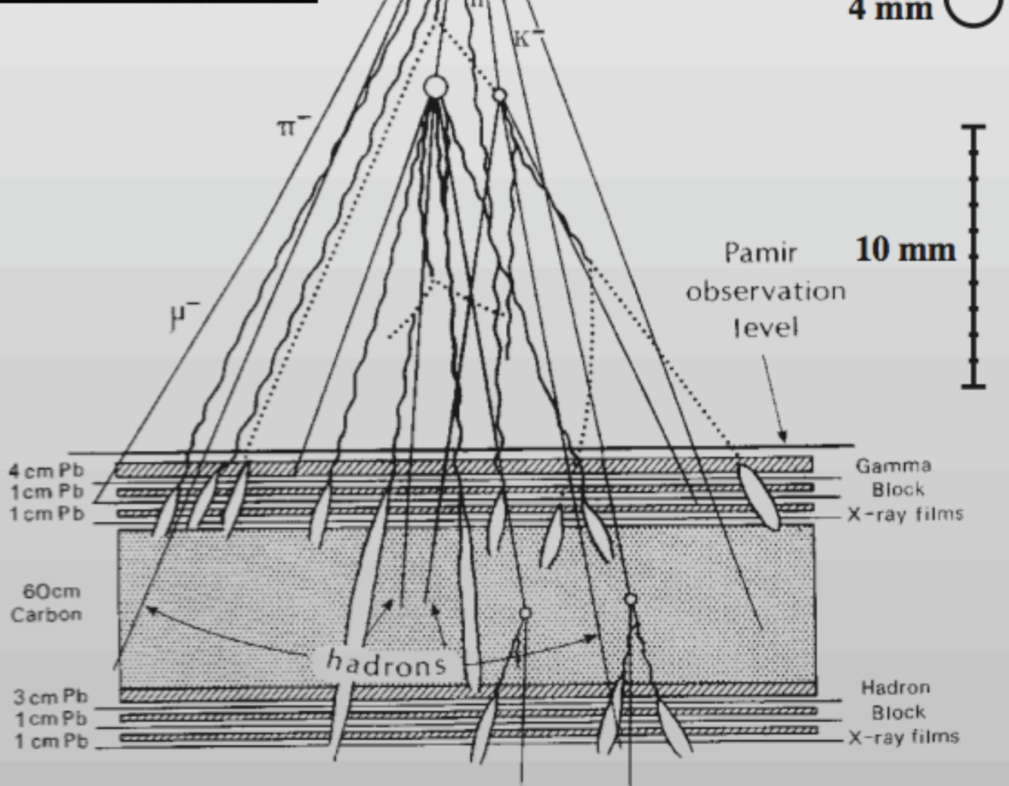

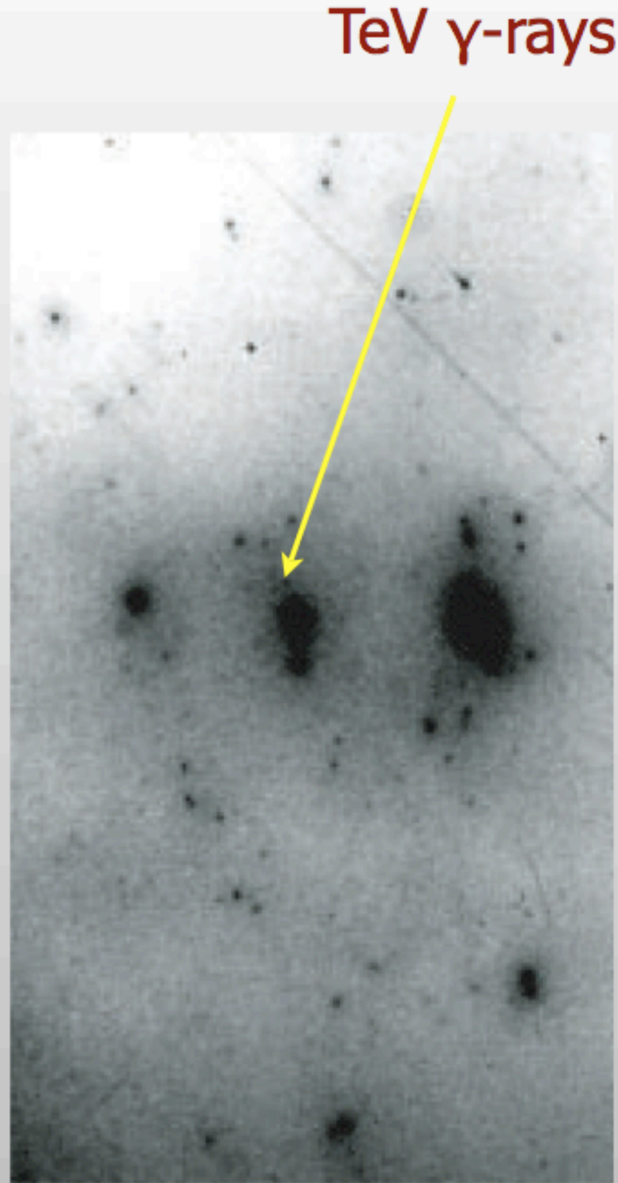

RUNJOB – Emulsion Chamber on Balloon

Gamma rays from first interaction detected

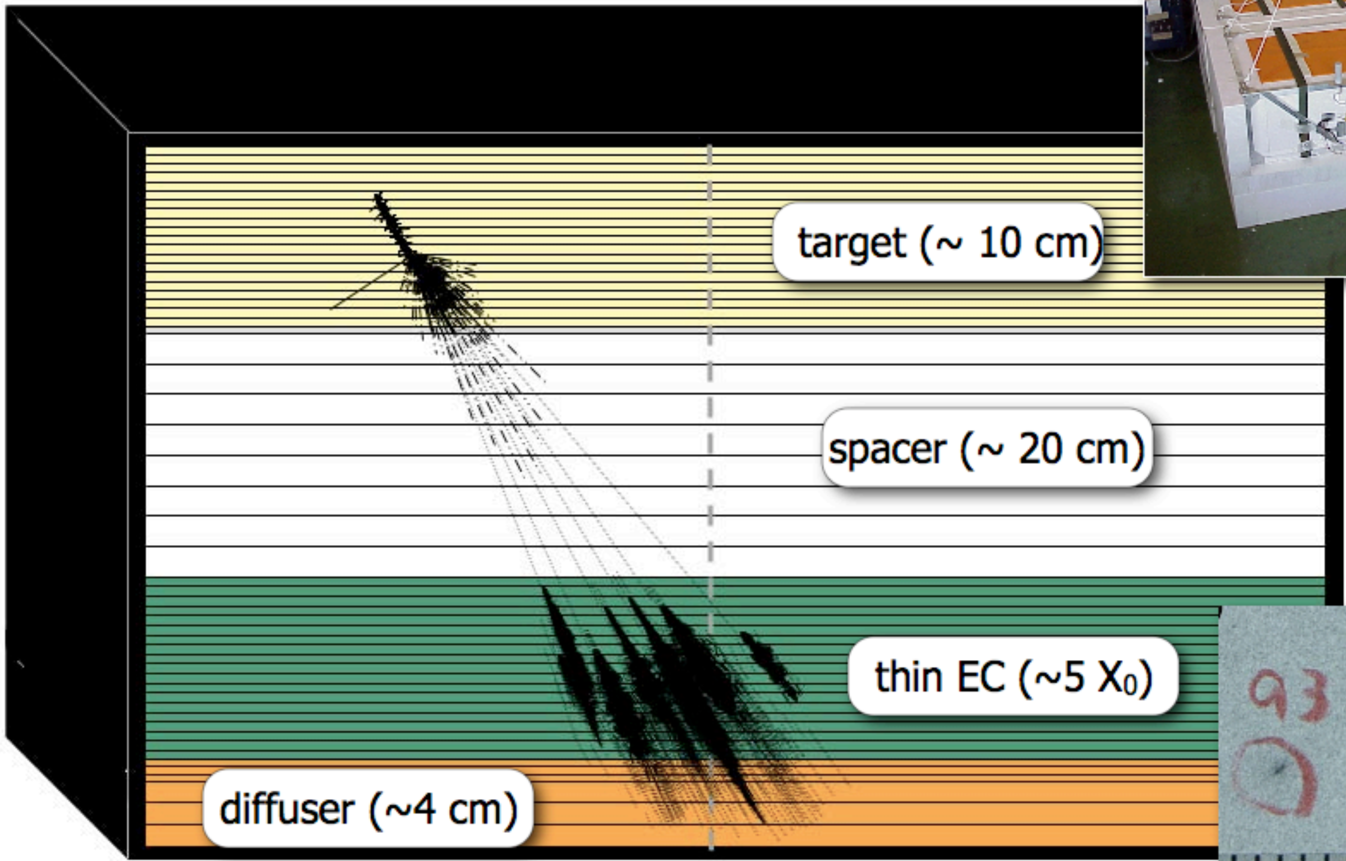

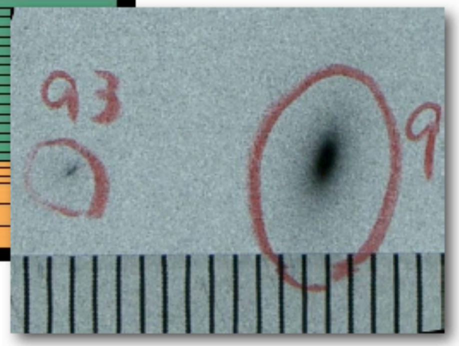

A = 0.4 m^2; obs. time: 1437.5 h; exposure 575 m^2h

RUNJOB e.m. calorimeter

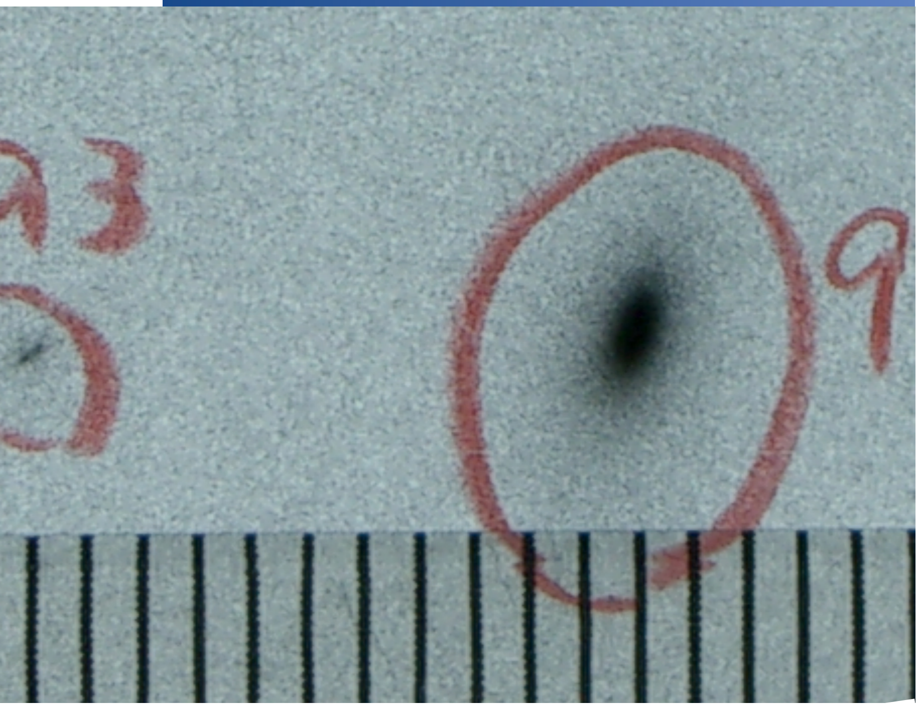

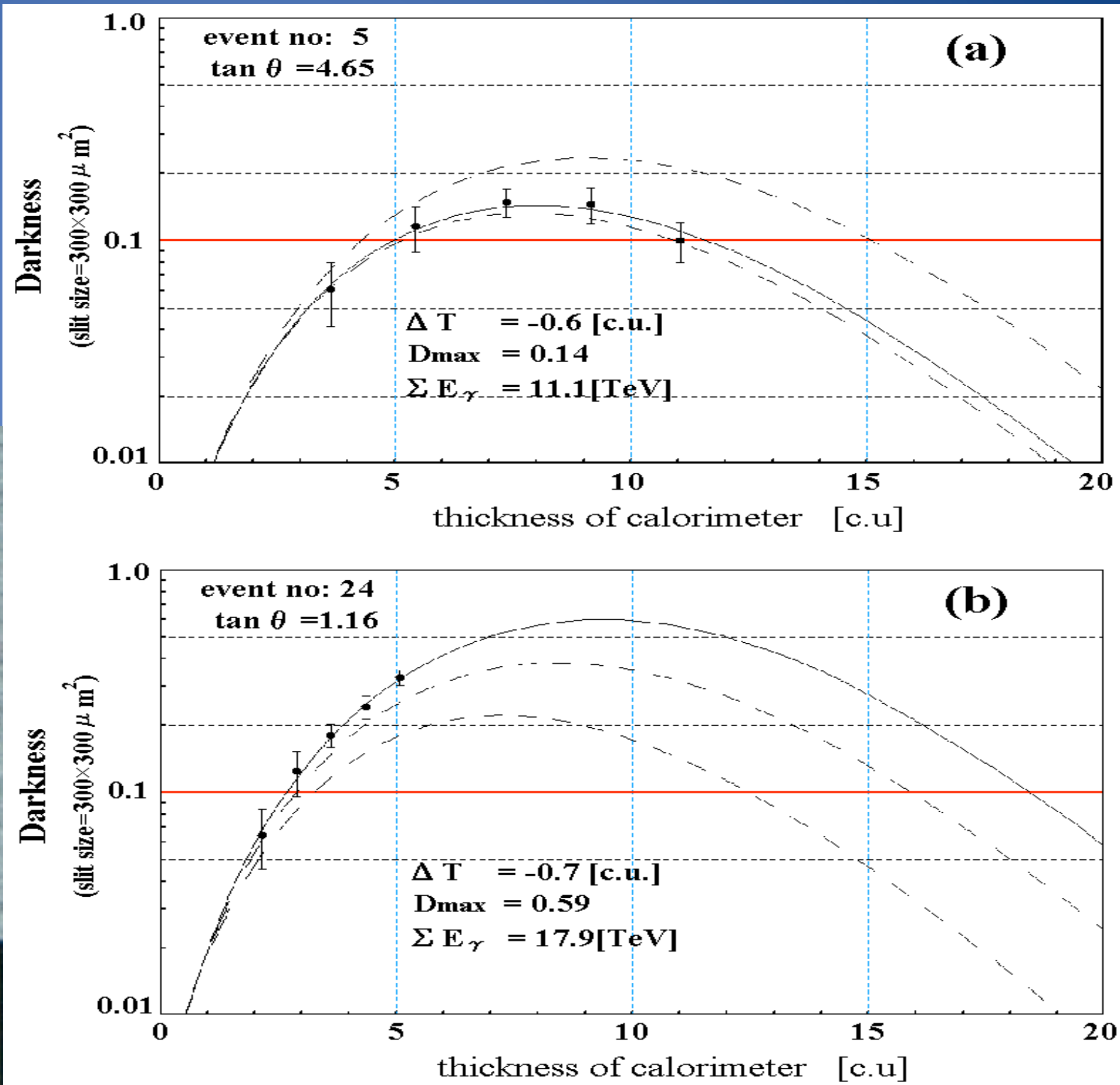

Energy resolution of γ- core method

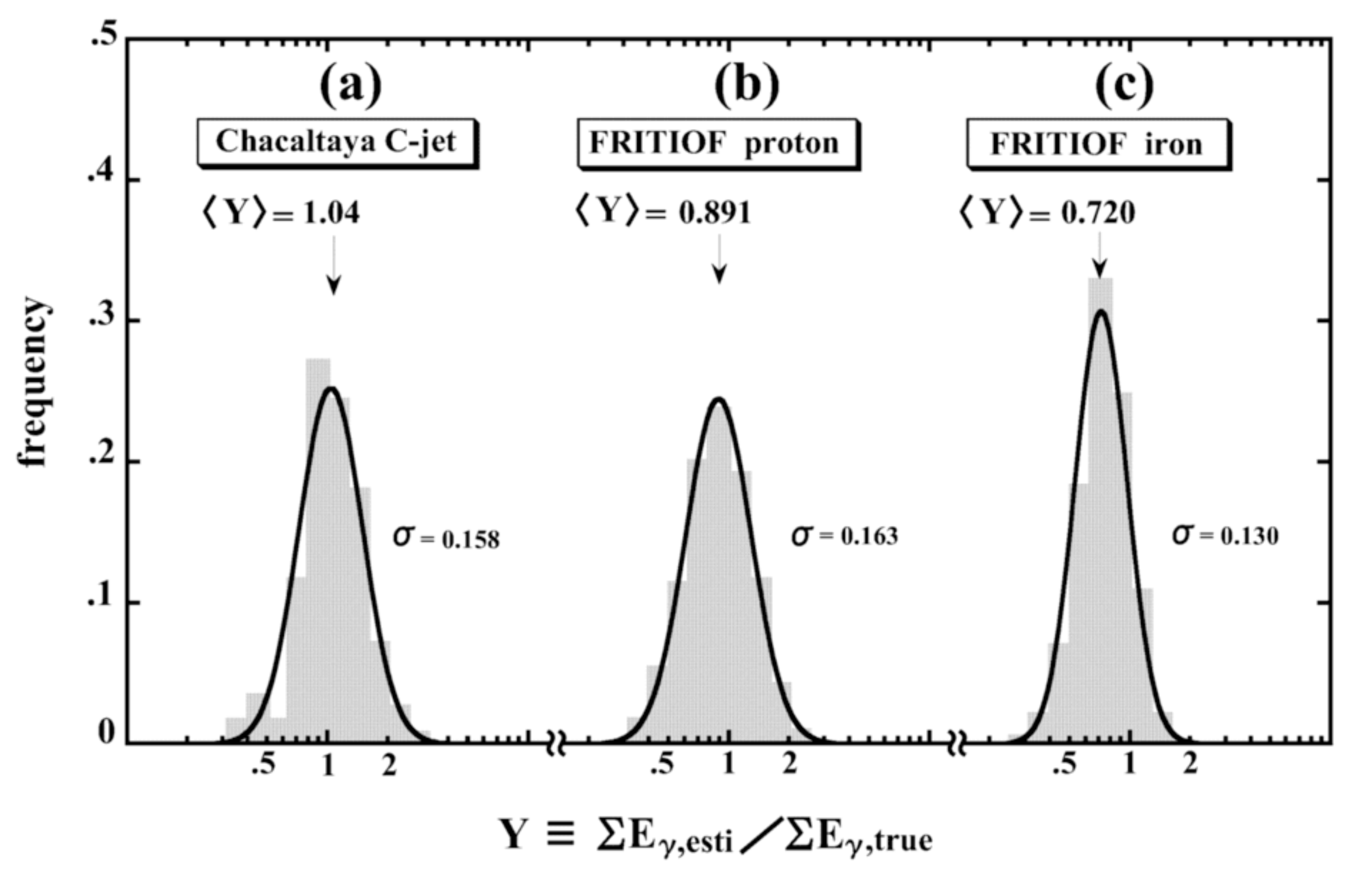

Conversion from shower energy to primary energy kγ: fraction of energy transferred to photons in first interaction

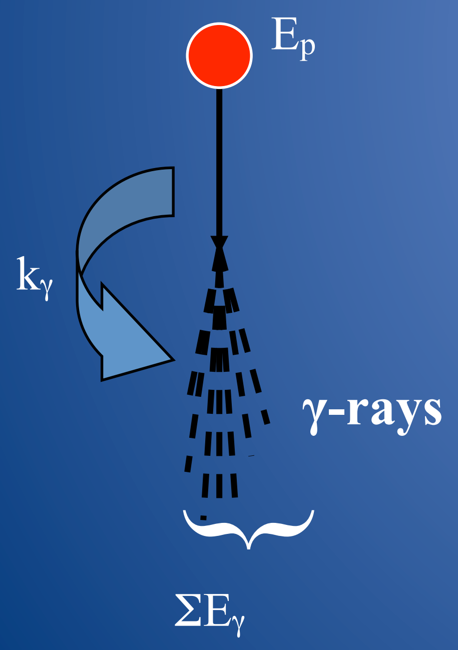

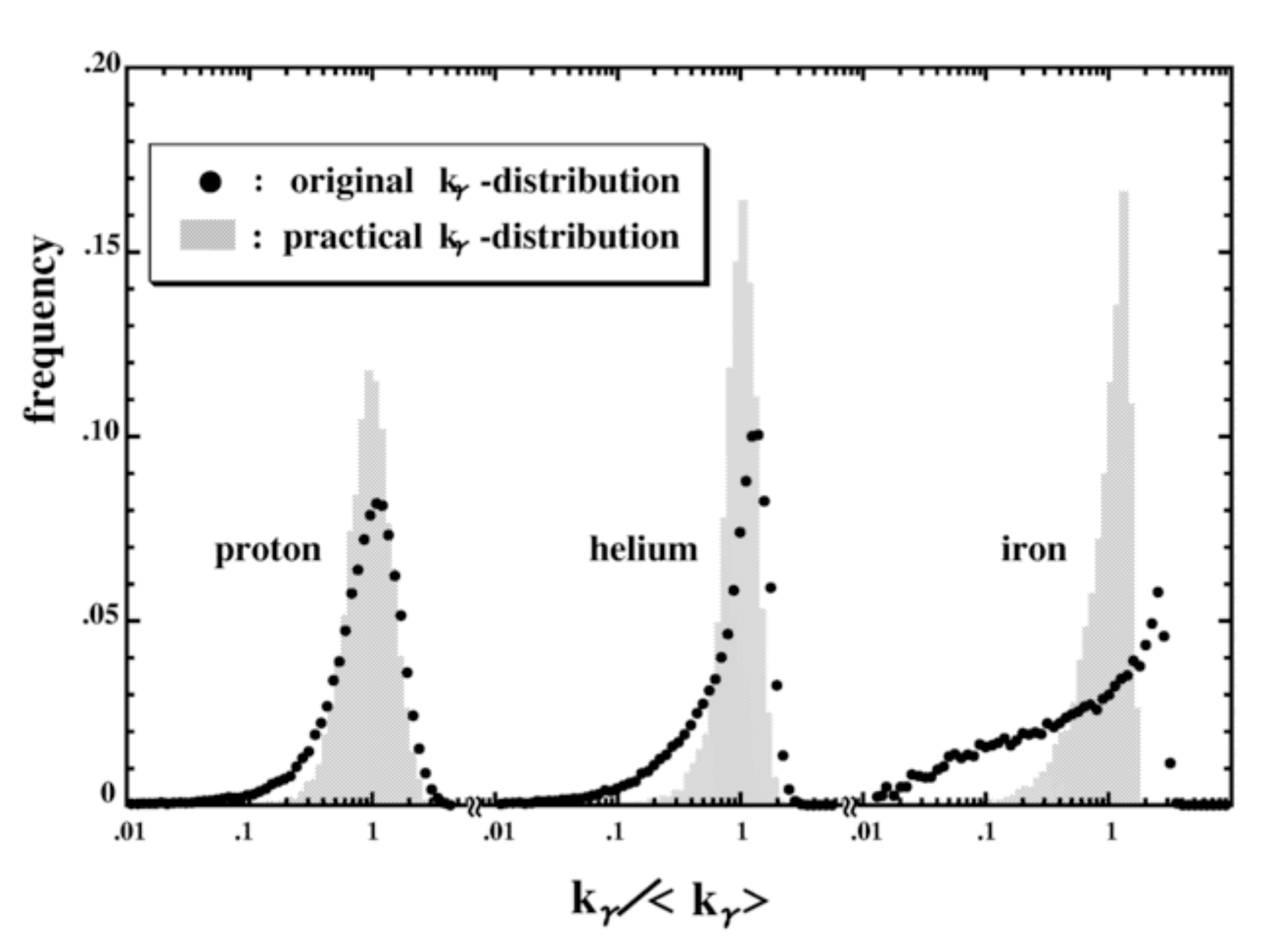

Charge determination in RUNJOB

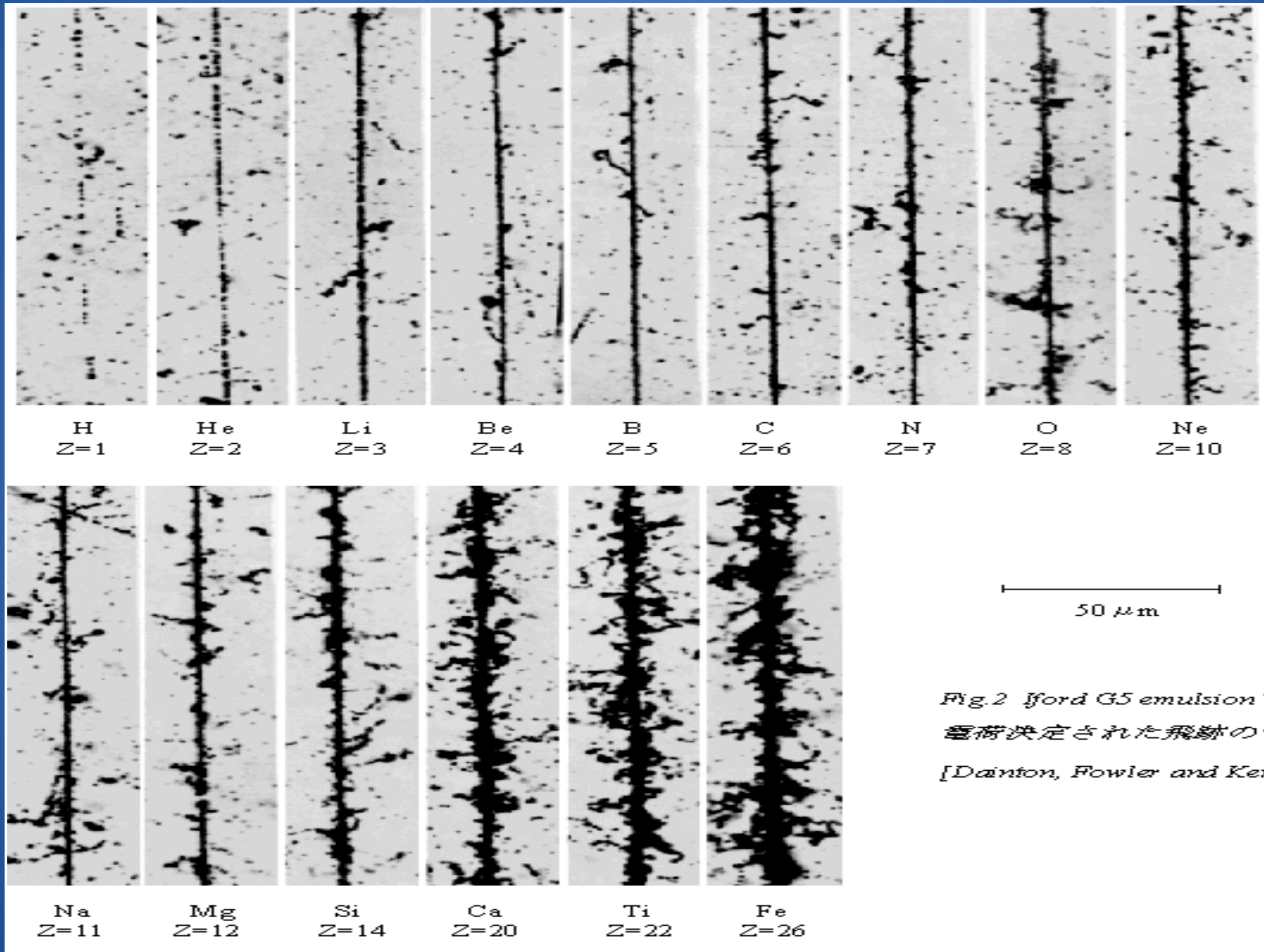

Fig.2 Ilford G5 emulsion で
電荷決定された飛跡のサンプル
[Dainton, Fowler and Kent (1952)]

Charge resolution

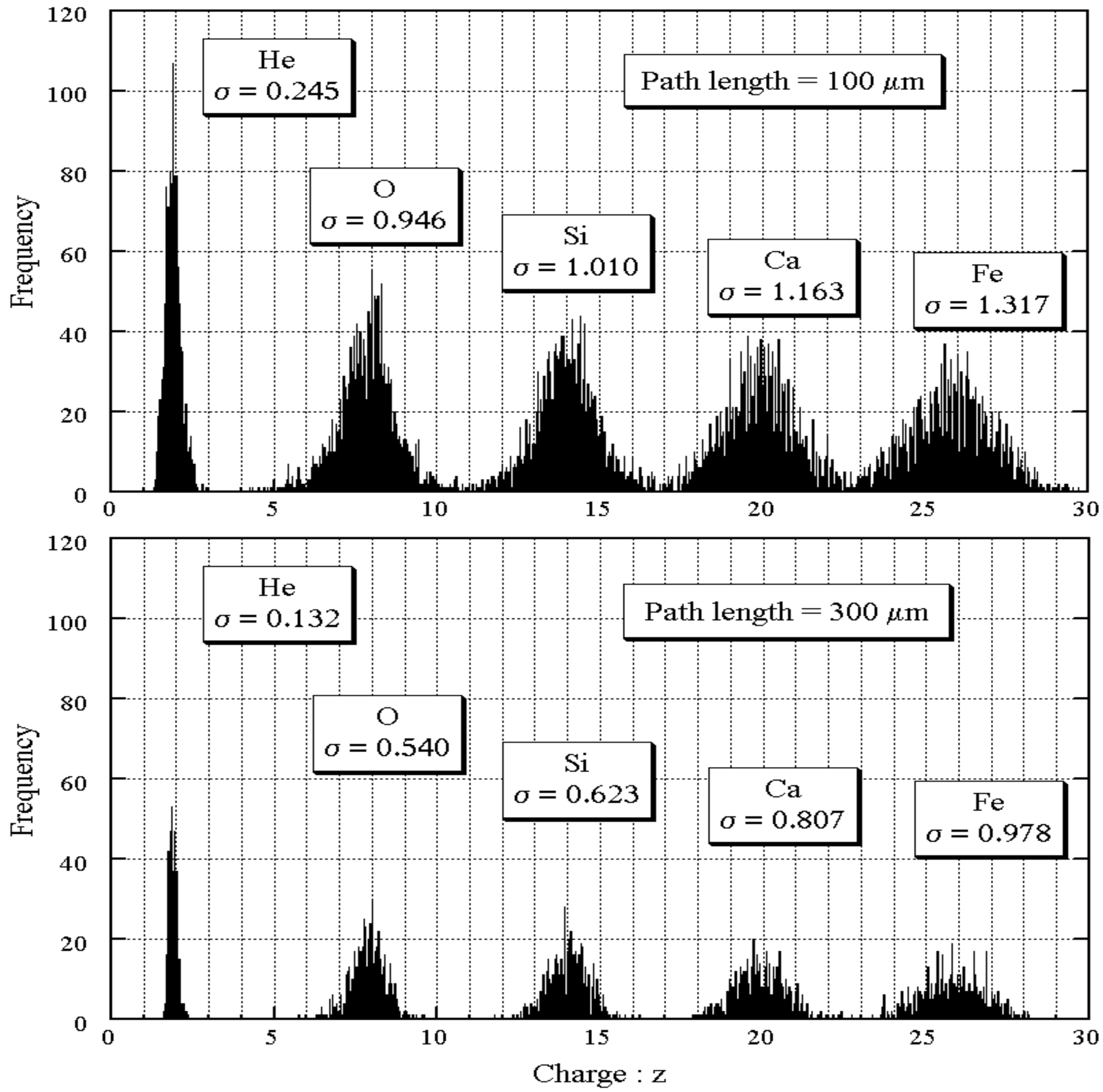

Fig. 5.5b シミュレーション計算による電荷分解能(2)

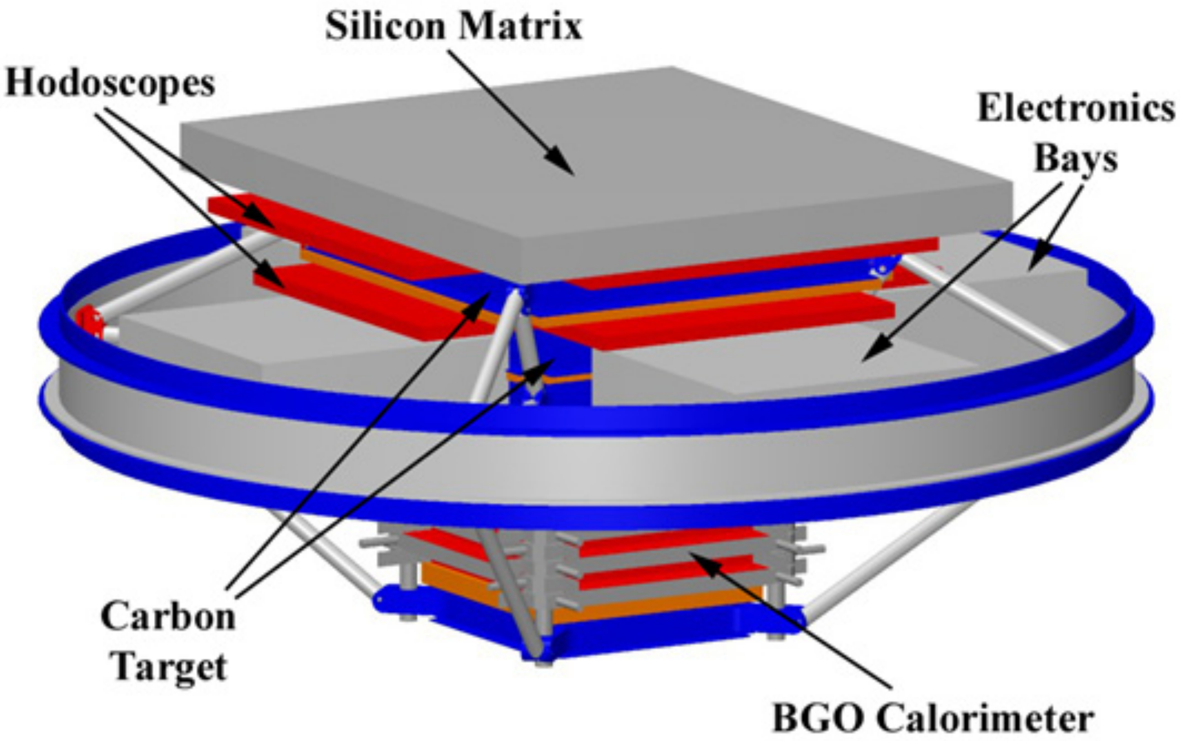

New space detectors ATIC

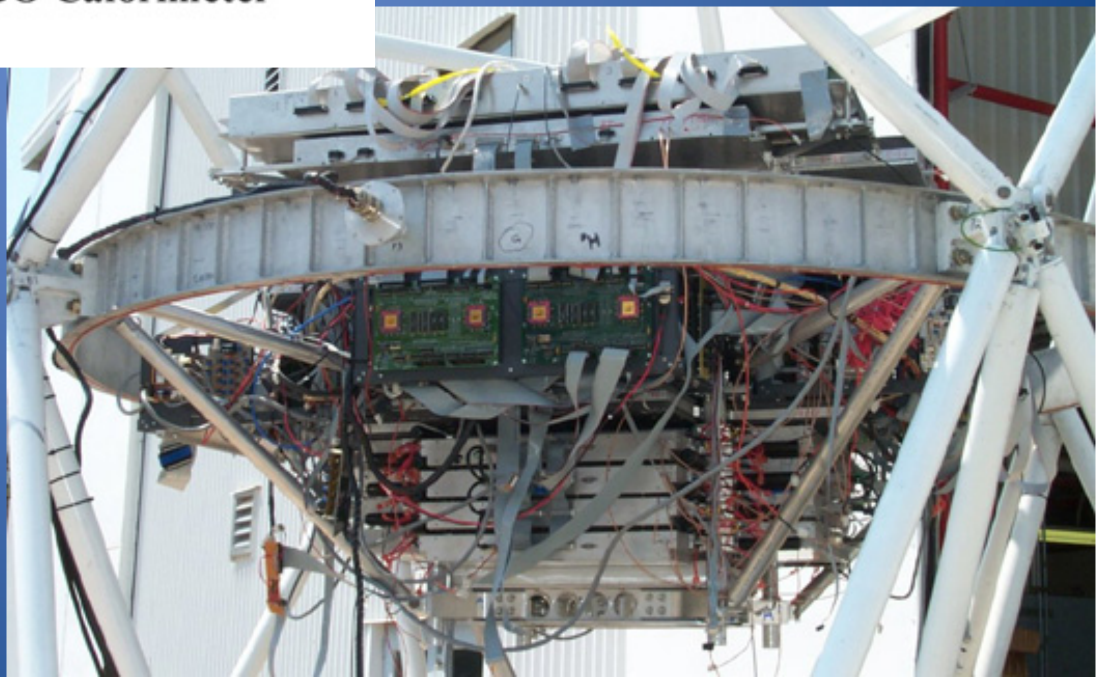

Long duration flights
In Antarctica

ATIC Instrument Details

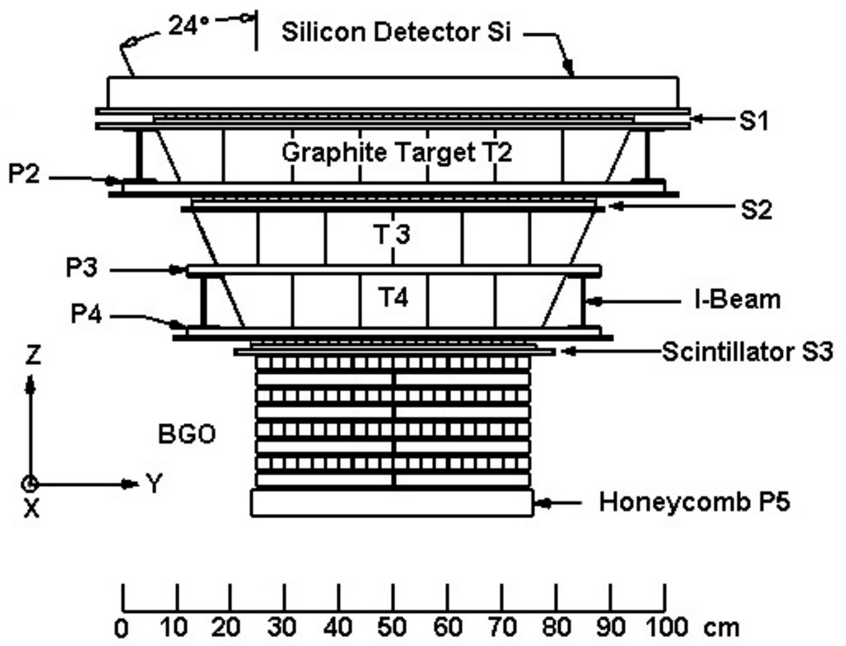

- **Si-Matrix:** 4480 pixels each 2 cm x 1.5 cm mounted on offset ladders; 0.95 m x 1.05 m area; 16 bit ADC; CR-1 ASIC's; sparsified readout.
- **Scintillators:** 3 x-y layers; 2 cm x 1 cm cross section; Bicron BC-408; Hamamatsu R5611 pmts both ends; two gain ranges; ACE ASIC. S1 – 336 channels; S2 – 280 channels; S3 – 192 channels; First level trigger: S1-S3
- **Calorimeter:** 8 layers (10 for ATIC-3); 2.5 cm x 2.5 cm x 25 cm BGO crystals, 40 per layer, each crystal viewed by R5611 pmt; three gain ranges; ACE ASIC; 960 channels (1200 for ATIC-3).

Data System: All data recorded on-board; 70 Gbyte disk (150 Gbyte for ATIC-3); LOS data rate – 330 kbps; TDRSS data rate – 4 kbps (6+ kbps for ATIC-3); Underflight capability (not used).

Housekeeping: Temperature, Pressure, Voltage, Current, Rates, Software Status, Disk status

Command Capability: Power on / off; Trigger type; Thresholds; Pre-scaler; Housekeeping frequency; LOS data rate, Reboot nodes; High Volt settings; Data collection on / off

Geometry Factors: S1-S3: 0.42 m^2sr; S1-S3-BGO 6: 0.24 m^2sr; S1-S3-BGO 8: 0.21 m^2sr

ATIC Instrument Summary

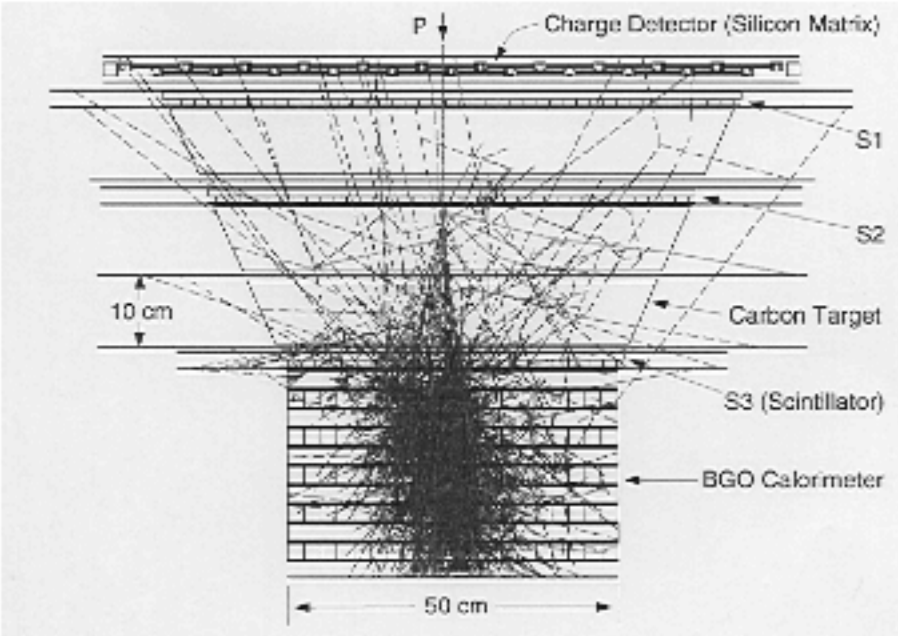

- Measure charge, energy and number
- Ionization Calorimetry only practical method to measure high energy light elements
- Silicon Matrix (Si) has 4,480 pixels to measure GCR charge in presence of shower backscatter
- Graphite Target to interact the primary particle and generate fragments that, in turn, will start an electromagnetic cascade. Also provides some backscatter shielding
- Plastic scintillator hodoscopes (S1, S2, S3) , embedded in Carbon target, provides event trigger plus charge & trajectory information
- Fully active calorimeter includes 400 Bismuth Germinate (BGO) crystals to foster and measure the nuclear - electromagnetic cascade showers
- Geometrical factor: 0.24 m^2sr (S1 – S3 – BGO6)

ATIC has been extensively simulated

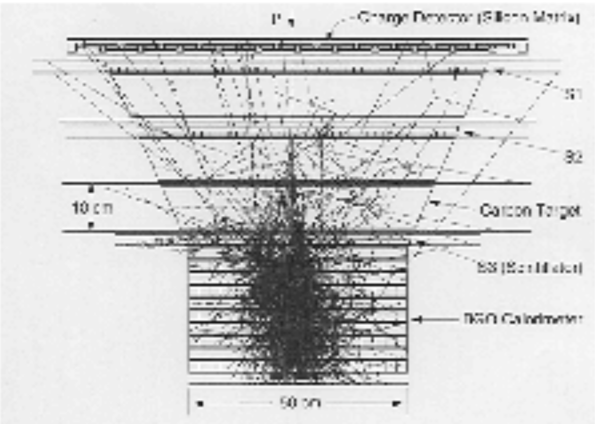

An example of a proton shower in the McMurdo flight configuration

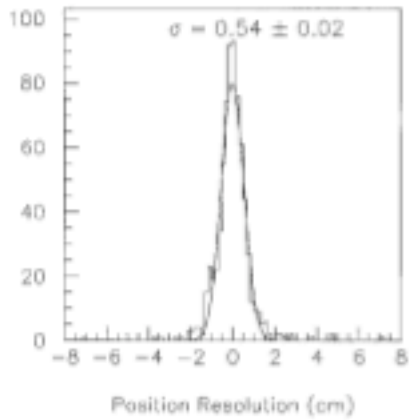

Trajectory resolution in S1 calculated from the BGO shower profile for 1 TeV protons.

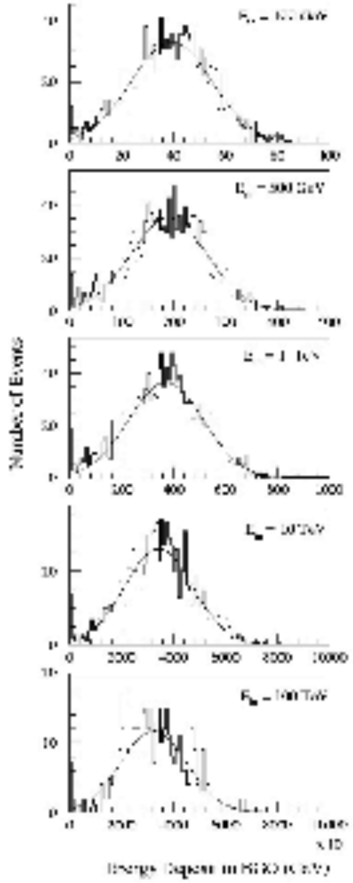

Energy deposition in 20 cm depth BGO calorimeter for 10^2, $5x10^2$, 10^3, 10^4, and 10^5 GeV protons.

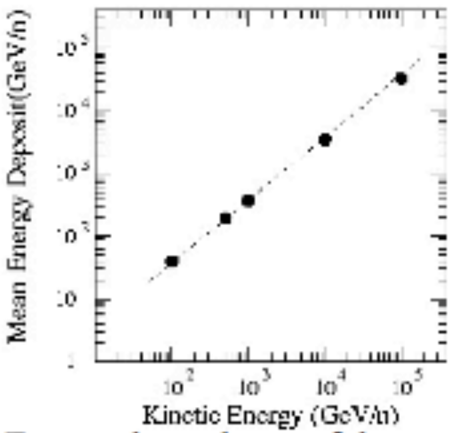

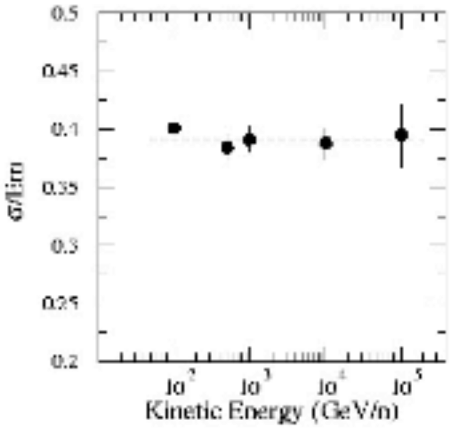

40%

Energy dependence of the proton mean energy deposit and the energy resolution.

Charge resolution in the p-He group

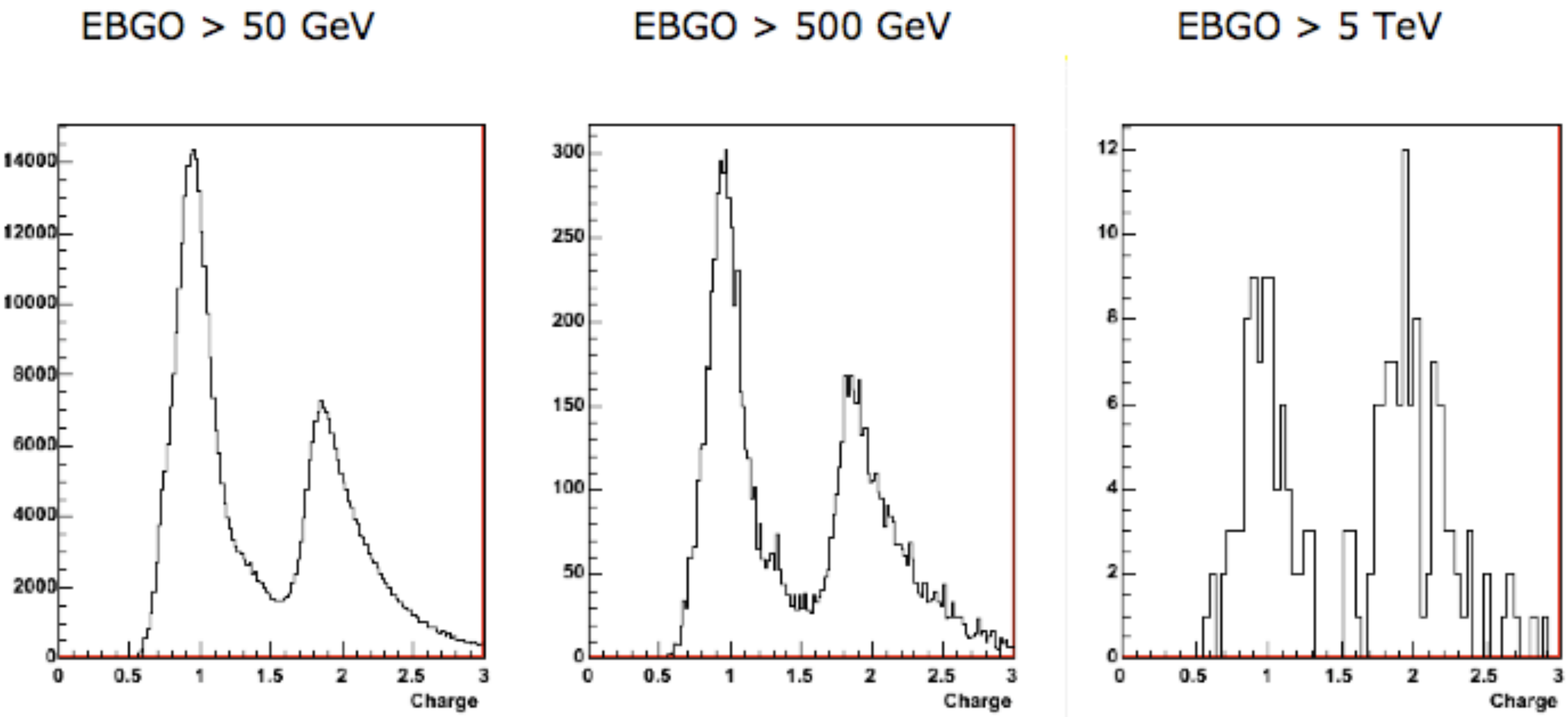

Antarctica long duration flights

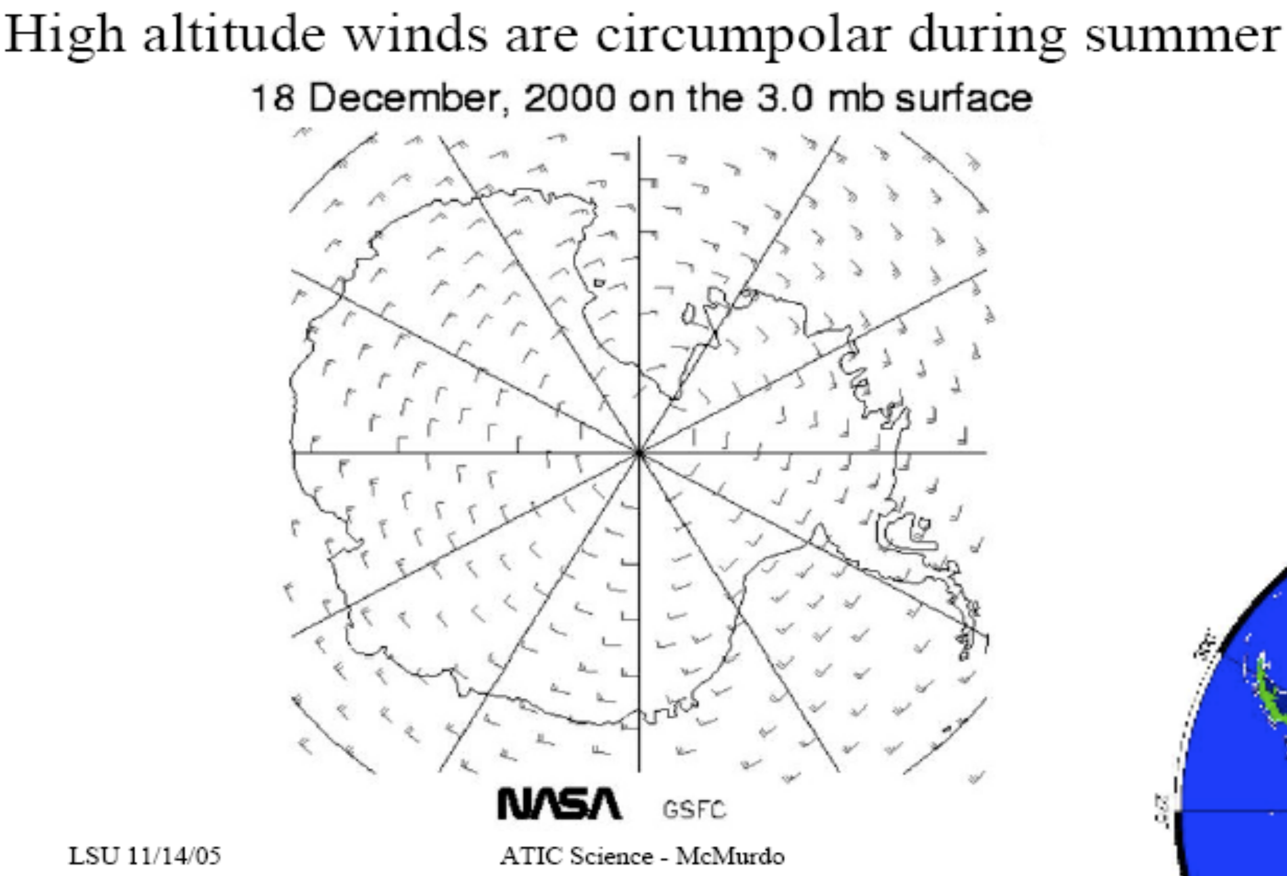

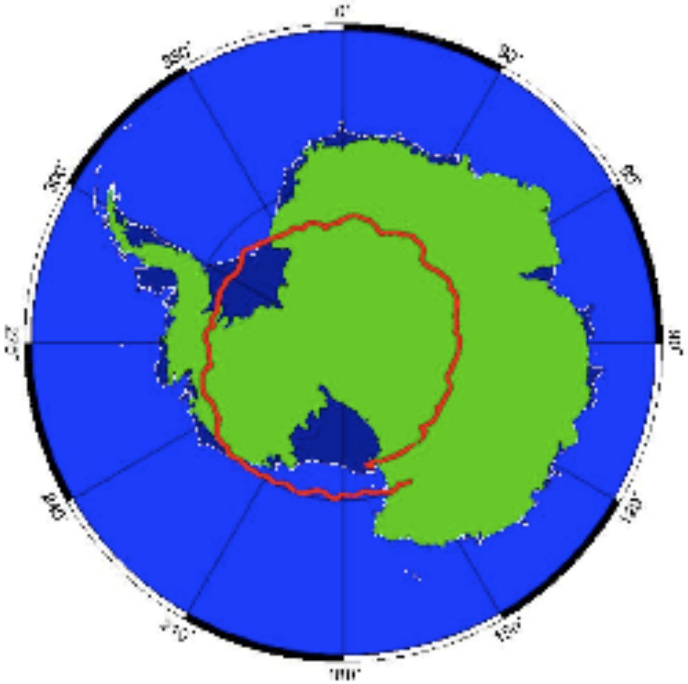

Flight and Recovery

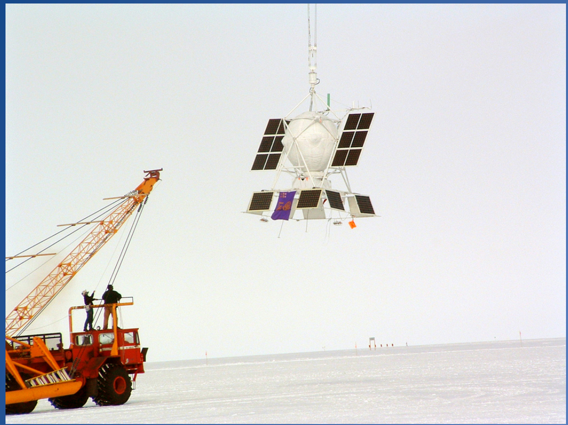

Launch of ATIC-2 in Dec. 2002

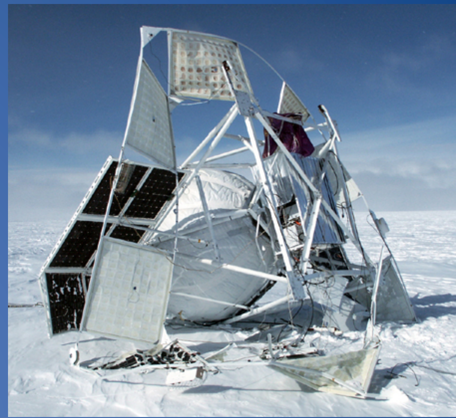

The good ATIC-1 landing on 1/13/01 (left) and the not so good landing of ATIC-2 on 1/18/03 (right)

ATIC is designed to be disassembled in the field and recovered with Twin Otters. Two recovery flights are necessary to return all the ATIC components. Pictures show 1st recovery flight of ATIC-1

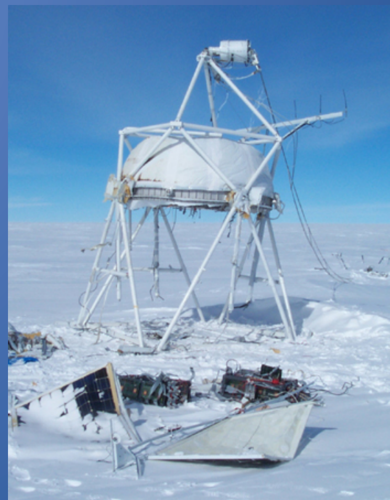

CREAM
(long balloon flights: 42/28 days)

•

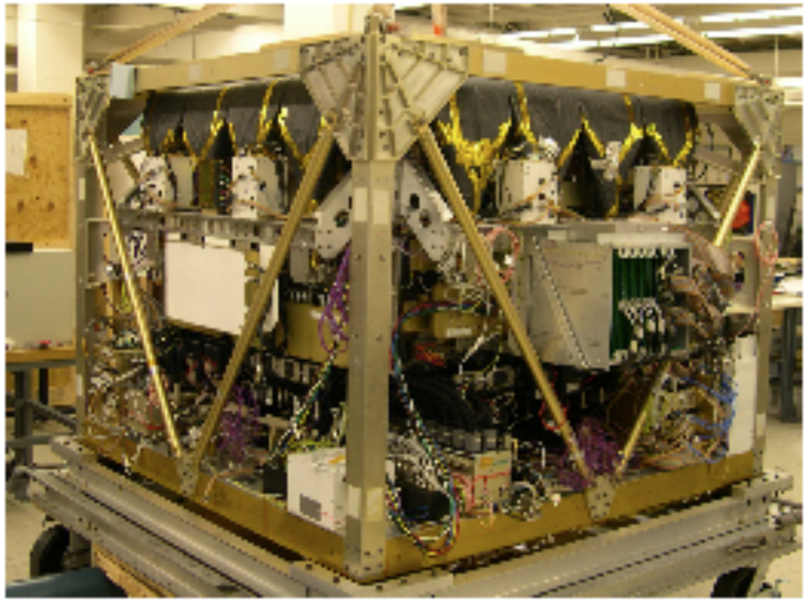

Figure 1. Photo of the CREAM Instrument during integration.

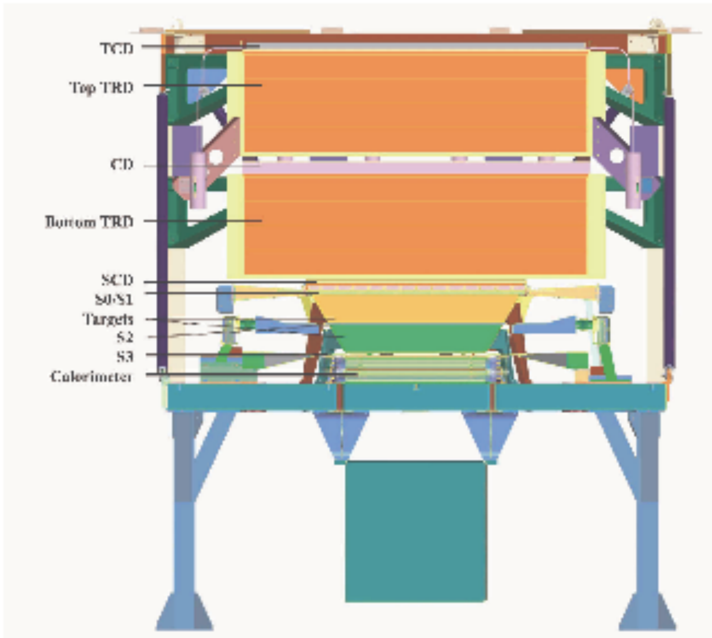

Figure 2. Schematic cross section drawing of major CREAM detector systems.

W = 1143 kg P = 379 W   dim = 180 x 180 x 128 cm^3
Acc = 0.3 m^2 sr (2xATIC)

Calorimeter: 20 Xo tungsten sampled every Xo;
sampling fraction 0.3% (scintillating fibers)

SEE YOU TOMORROW….

……. GROUND BASED DETECTORS